

THESIS

HYDROGEN-NATURAL GAS FUEL BLENDING AND ADVANCED AIR FUEL RATIO
CONTROL STRATEGIES IN A "RICH BURN" ENGINE WITH 3-WAY CATALYST

Submitted by

Nicholas Katsampes,

Department of Mechanical Engineering

In partial fulfillment of the requirements

for the Degree of Master of Science

Colorado State University

Fort Collins, Colorado

Fall 2023

Master's Committee:

Advisor: Daniel B. Olsen

Karen Thorsett-Hill

Sybil Sharvelle

Copyright by Nicholas Katsampes, 2023

All Rights Reserved

ABSTRACT

HYDROGEN-NATURAL GAS FUEL BLENDING AND ADVANCED AIR FUEL RATIO CONTROL STRATEGIES IN A "RICH BURN" ENGINE WITH 3-WAY CATALYST

Interest in hydrogen (H_2) fuels is growing, with industry planning to produce it with stranded or excess energy from renewable sources in the future. Natural gas (NG) utility companies are now taking action to blend H_2 into their preexisting pipelines to reduce greenhouse gas (GHG) emissions from burning NG. "Rich burn" (stoichiometric) engines with 3-way catalysts are not typically used with H_2 -NG blending; however, many of these engines operate on pipeline NG and will receive blended fuel as more gas utilities expand H_2 production. These engines are typically chosen for their low emissions owing to the 3-way catalyst control, so the focus of this paper is on the change in emissions like carbon monoxide (CO) and nitrogen oxides (NO_x) as the fuel is blended with up to 30% H_2 by volume. The Caterpillar CG137-8 natural gas engine used for testing was originally designed for industrial gas compression applications and is a good representative for most "rich burn" engines used across industry for applications such as power generation and water pumping.

Results indicate a significant reduction in greenhouse gas (GHG) emissions as more H_2 is added to the fuel. Increasing H_2 in the fuel changes combustion behavior in the cylinder, resulting in faster ignition and higher cylinder pressures, which increase engine-out NO_x emissions. Pre-catalyst emissions behave as expected; CO decreases and NO_x increases. Unexpectedly, post-catalyst CO and NO_x both decrease slightly with increasing H_2 while operating at the optimal "air-fuel" equivalence ratio (λ or "lambda"). This testing shows that a "rich burn" engine with 3-way catalyst can tolerate up to 30% H_2 (by vol.) while still meeting

NO_x and CO emissions limits. However, this research found that at elevated levels of H₂, increased engine-out NO_x emissions narrow the λ range of operation. As H₂ is added to NG pipelines, some “rich burn” engine systems may require larger catalysts or more precise λ control to tolerate the increased NO_x production associated with a H₂-NG blend.

This paper includes additional investigation into transitioning H₂ concentrations. Sudden step-increases in H₂ cause dramatic changes in λ , resulting in large emissions of post-catalyst NO_x during the transition. Comparable changes in H₂ at elevated concentrations cause larger spikes in NO_x than at lower concentrations. The amount of post-catalyst NO_x produced during a step-transition is influenced by the engine controller and how quickly it adapts to the change in λ . Better tuned engine controllers respond more quickly and produce less NO_x during H₂ step-transitions. This research shows that some engines can violate NO_x emissions limits with as little as a 5% increase in H₂ due to slow engine controller response.

ACKNOWLEDGEMENTS

I would like to acknowledge my appreciation for my graduate advisor, Dr. Daniel B. Olsen, for his patience and guidance throughout this endeavor. I feel lucky to have been a part of Dr. Olsen's research group at CSU.

I would also like to acknowledge my appreciation for Southern California Gas Company for funding this research and for providing additional support from a field application perspective. To Gregg Arney in particular, for his continuous communication and fantastic feedback at every step throughout the project.

I would also like to acknowledge my appreciation for Caterpillar Inc. for funding this research and for providing professional advice. Every interaction I've had with Caterpillar employees through this project has been positive as they tried to help resolve any issues we ran into. To Dr. Dave Montgomery in particular for his friendly outreach, expert advice, and for teaching industry knowledge at CSU.

Finally, and most importantly, I would like to acknowledge my appreciation for my family and friends during this experience. In particular, for my wife Paula and my parents Mike and Mary, I would not be where I am today without their unconditional love and support.

TABLE OF CONTENTS

ABSTRACT	ii
ACKNOWLEDGEMENTS	iv
CHAPTER 1: INTRODUCTION.....	1
1.1, Background and Motivation.....	1
1.2, Rich Burn Engines and 3-Way Catalysts	2
1.3, H ₂ -Natural Gas Blending.....	8
1.4, Research Objectives.....	10
CHAPTER 2: METHOD	13
2.1, Engine Test Cell and Air-Fuel Controls	13
2.2, Three-Way Catalyst and Emissions Sampling	16
2.3, Fuel Blending	18
2.4, Testing Procedure.....	20
CHAPTER 3: BASELINE TESTING AND OPERATION PARAMETER ANALYSIS	23
3.1, Spark Timing Exploration.....	23
3.2, Baseline λ -Sweep.....	24
3.3, Dithering Technique	28
CHAPTER 4: HYDROGEN FUEL BLENDING	32
4.1, Hydrogen Fuel Concentration Sweep.....	32
4.2, λ -Sweep with 20% H ₂ Blend	38
4.3, H ₂ Concentration Transitions.....	40
4.4, LECM Response Time (PID).....	45
CONCLUSION	54

REFERENCES.....	57
APPENDICES.....	61

CHAPTER 1: INTRODUCTION

1.1, Background and Motivation

Spark ignited stoichiometric (“rich burn”) natural gas engines with 3- way catalysts are known for having low emissions of nitrogen oxides (NO_x), carbon monoxide (CO), and unburned hydrocarbons (THCs). These engines only achieve their superior emissions performance by operating in a narrow range of “air-fuel” equivalence ratio (λ or "lambda") for the 3-way catalyst to reduce NO_x and CO emissions. The goal of this research is to observe the changes in emissions as hydrogen gas (H₂) is blended into the natural gas (NG) fuel supply of a rich burn engine set, as well as to explore λ control techniques to improve catalyst effectiveness.

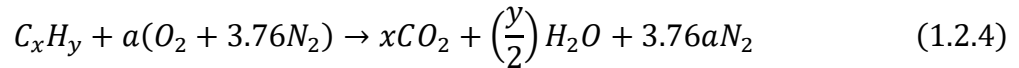
Interest in H₂ fuel blending is rising as a solution to substitute hydrocarbon fuel and thus reduce carbon emissions. The US Department of Energy is funding many initiatives working towards this goal, with \$9.5 billion dollars set aside for clean H₂ initiatives in a new infrastructure law released in 2022 [1]. Hydrogen blending in natural gas pipelines is being explored as a way to transport H₂ fuel on a large scale. The US department of Energy’s Hyblend initiative was created to provide up to \$15 million dollars in funding toward this goal [2].

Southern California Gas, a Sempra company and the largest natural gas distribution utility in the US has stated their mission to reach net zero greenhouse gas emissions by the year 2045 [3]. In 2020 they set up a H₂ blending demonstration program to verify the integrity of distribution systems with the goal of blending up to 20% H₂ into pipeline natural gas [4]. This demonstration program is intended to benefit customers by showing the expected effects of H₂ addition in polyethylene and steel piping, as well as in combustion equipment. As part of this program, SoCal Gas partnered with CSU’s Engines and Energy Conversion Laboratory to

investigate the effects of H₂ blending in a rich burn engine with a 3-way catalyst. The purpose of this research project was to assess the impact on emissions from these engine sets with H₂ blending, and to explore and demonstrate advanced air-fuel ratio control techniques.

1.2, Rich Burn Engines and 3-Way Catalysts

All combustion engines using air and fuel must consider their air-fuel ratio (AFR). The “stoichiometric” AFR is the theoretical ratio where there is just enough air present to fully oxidize all of the fuel without any reactants remaining. The stoichiometric AFR is different for each fuel in question, and changes when the mixture of fuel constituents change. The stoichiometric relation for a given fuel represented as C_xH_y is shown below in equation (1.2.4).



$$\text{where } a = x + y/4$$

Shown in equation (1.2.5), AFR is typically a mass-based ratio. The stoichiometric AFR can be found using the coefficient “*a*” from equation (1.2.4) and the molecular weights of the air and fuel, shown below in equation (1.2.6) [5].

$$AFR = \frac{mass_{air}}{mass_{fuel}} \quad (1.2.5)$$

$$(AFR)_{stoich} = 4.76a \frac{MW_{air}}{MW_{fuel}} \quad (1.2.6)$$

“Equivalence ratio” is an air-fuel parameter used in practice as a comparison of the actual operating AFR to the stoichiometric AFR. In this paper, we will use the “air-fuel” equivalence ratio (“lambda” or λ, sometimes called the “excess air coefficient”), shown in equation (1.2.7). Further discussion on the ratio of air to fuel supplied to the engine will be in terms of λ, where

$\lambda=1$ is stoichiometric, $\lambda<1$ has excessive fuel (a rich mixture), and $\lambda>1$ has excessive air (a lean mixture), visual representation in Figure 1.2.1.

$$\lambda = \frac{AFR_{actual}}{AFR_{stoich}} = \frac{1}{\Phi} \quad (1.2.7)$$

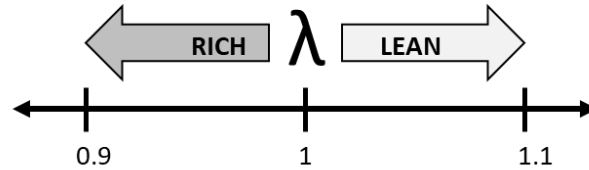


Figure 1.2.1. Visual representation of λ pertaining to lean and rich mixtures.

Two common emissions of concern from spark-ignited engines are NO_x and CO. Nitrogen Oxides (NO_x), consisting of nitric oxide (NO) and nitrogen dioxide (NO₂), are typically produced when the engine runs lean. Described as the Zeldovich mechanism, when combustion in the cylinder gets too hot and excess O₂ is present, then N₂ from the air will dissociate and bond with oxygen forming NO_x [5]. Once in the atmosphere, NO_x will bond with volatile organic compounds (VOCs) to form ozone (O₃), a known smog gas that is harmful to breath [6]. On the other hand, carbon monoxide (CO) is typically produced when the engine runs too rich. Ideally, there would be enough oxygen present oxidize all of the CO completely into CO₂, however when there is not enough oxygen then the carbon is left as CO, a gas known to be harmful to breath.

There are two main approaches to operating spark-ignited engines with low emissions, lean burn and stoichiometric burn (AKA “rich burn”). Both engine types are designed for maximum reduction of emissions, particularly NO_x, CO, and unburned hydrocarbons (HCs). The approach for lean burn engines is to dilute the air-fuel mixture with excess air, producing low emissions directly from the engine and needing little aftertreatment. “Rich burn” engines, however, operate with nearly stoichiometric proportions of air and fuel for combustion, and

produce considerably more NO_x and CO in their exhaust than lean engines. “Rich burn” engines compensate by using 3-way catalysts with non-selective catalytic reduction (NSCR) to reduce NO_x, CO, and HCs to acceptable levels. A visual comparison between stoichiometric and lean engines and their relative exhaust emissions is shown in Figure 1.2.2.

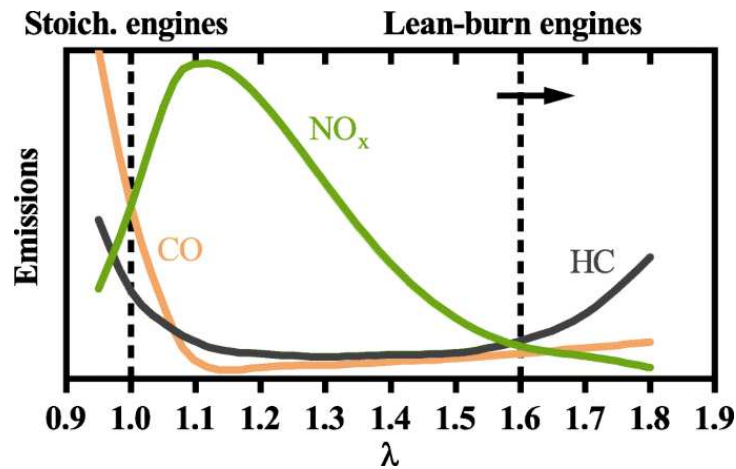


Figure 1.2.2. A simplified plot comparing emissions produced by stoichiometric and lean burn engines. Image source from [7].

The 3-way catalysts used with “rich burn” engines are very effective at reducing these emissions to incredibly low levels, making “rich burn” engine-sets the best choice for minimal emissions [8]. This can be counterintuitive, because lean burn engines produce low emissions in their exhaust, while “rich burn” engines produce high emissions in their exhaust but reduce them using the catalyst. “Rich burn” engines with catalysts are very common in the automotive industry, typically calling the catalyst the “catalytic converter” [9], however they are relatively new in the industrial natural gas sector.

The reason 3-way catalysts are effective on “rich burn” engines is because they use NO_x and CO from the exhaust to convert each other, reducing NO_x into N₂ and oxidizing CO and HCs into CO₂. Representative chemical balances are shown below in equations (1.2.1), (1.2.2), and (1.2.3) [10]. Three-way catalysts function by pulling oxygen atoms away from NO_x

molecules and providing them to the CO molecules, so maintaining the proportion of NO_x to CO is essential for proper catalyst function. The third action of 3-way catalysts is to oxidize as much remaining unburned hydrocarbon fuel (THC) as possible, by using whatever oxygen remains after oxidizing the CO present. A basic visual representation of the exchange between NO_x and CO in the 3-way catalyst is shown below in Figure 1.2.3.

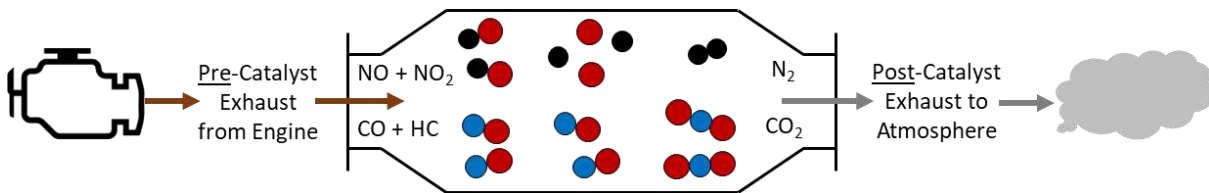
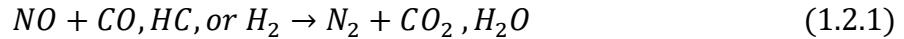


Figure 1.2.3. Basic visualization of NO_x and CO converting each other in the 3-way catalyst.

The chemistry makeup of the exhaust products supplied to the catalyst are directly controlled by the proportions of air and fuel supplied to the engine. When too much air is supplied to the engine, then excess air will be present in the exhaust. When this happens, the catalyst will pull oxygen atoms from the excess O₂ molecules instead of from NO_x, allowing large quantities of NO_x to pass through unaffected. Conversely, when too much fuel is supplied to the engine, then there is excess carbon left unoxidized. This produces large amounts of CO that the catalyst is unable to oxidize, allowing CO to pass through unaffected. The takeaway here, is that “rich burn” engines with 3-way catalysts “operate in tight ranges of air-fuel (A/F) ratios, where small variations have large effects on the emissions [11]” because the catalyst requires exact proportions of NO_x and CO.

Catalyst conversion efficiency describes how efficient the catalyst is at eliminating certain emissions. An example of catalyst conversion efficiency is shown in Figure 1.2.4 from a gasoline engine with catalyst [10]. Notice that there is only a small area called the “high performance region” where the catalyst is effectively converting all 3 emissions of concern. This region will be referred to as the “window of operation” or “window of compliance” in this paper, as the engine must operate within this region to stay under regulation emissions limits.

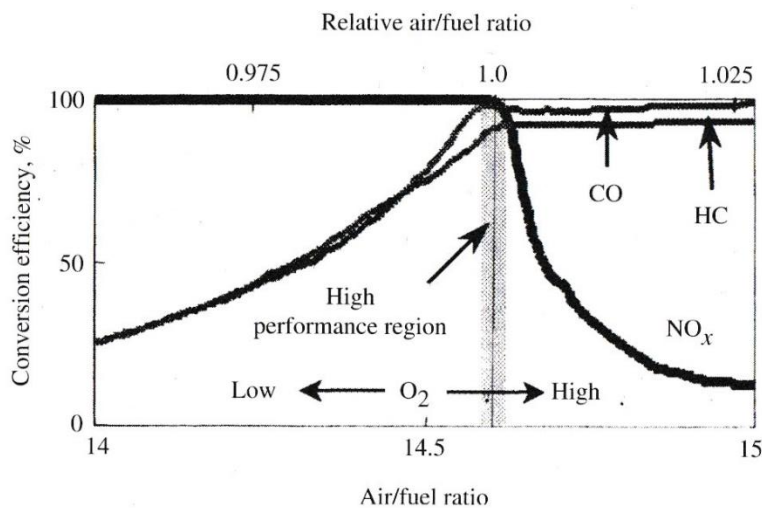


Figure 1.2.4. Catalyst conversion efficiency for a gasoline engine with 3-way catalyst.

The importance of air and fuel proportions with 3-way catalysts shows that improving control over air and fuel is an effective path for reducing emissions from rich burn engine sets. The two basic types of engine controls are open-loop and closed-loop control. Open-loop control is where the engine controller sends signals to equipment like the throttle valve or spark plugs without considering feedback. Open-loop systems typically operate with memory-based control systems, where optimal setpoints are preprogrammed into the engine controller [10]. These memory-based systems are disadvantaged as they are not capable of responding to changing conditions like equipment variations and fuel changes.

The better way to control the engine is to use an “adaptive control system” using closed-loop control. In this case, the engine controller sends signals to equipment then considers feedback from sensors on the engine and adjusts that signal to compensate. This can be direct feedback from the equipment, like sending a signal to the throttle valve and the valve gives feedback to the controller on its actual position. This can also be indirect feedback, like sending a signal to the throttle valve and the engine controller considers feedback from the intake manifold pressure sensor to maintain intake pressure. “Advanced” engine controllers are adaptive and capable of closed-loop control. New advanced controllers are often capable of more complex operations like switching between closed- and open-loop operation or referencing tables with different operating parameters depending on the conditions.

Traditionally, many older engines operate with memory-based systems where the fuel type is assumed, resulting in an air-fuel system that cannot adapt to changing fuel constituents. Most newer engines now come with engine controllers capable of closed-loop control over the air-fuel mixture. Most “rich burn” engines made today consider feedback from an Exhaust Gas Oxygen (EGO) sensor, often called the λ -sensor because it detects the presence of excess air in the exhaust [9]. Simple engine controllers will use an EGO sensor in a closed feedback loop, allowing the engine to adjust fuel and air flows to their ideal proportions by considering how much air is left over in the exhaust. Advanced controllers are becoming more available now, allowing for more complicated control techniques using various λ values for different loads, or using multiple EGO sensors placed before and after the catalyst.

Dithering is an advanced λ control technique where λ is fluctuated between rich and lean, providing the catalyst with short bursts of excess oxygen and excess CO, and it is intended to improve catalyst conversion efficiency. Research on this topic has been carried out previously at

CSU's Engines and Energy Conversion Laboratory by Defoort et al. in 2003 with focus on ammonia generation [11], and again in 2020 by A. Jones experimenting on the CG137-8 engine [12].

1.3, H₂-Natural Gas Blending

A goal of this research was to examine the changes in exhaust chemistry as H₂ is blended with natural gas fuel in a rich burn engine. These engines are not currently targeted for H₂-NG blending, with lean burn engines taking most of the attention because they are more widely used on NG pipelines. However, many rich burn engine-sets operate using pipeline natural gas fuel in areas with tighter emissions regulations, like inside cities. When H₂ is eventually blended into large natural gas pipeline networks, these rich burn engine sets will need to run with the new fuel blend while still meeting emissions limits.

The largest change to expect with H₂ will be in-cylinder combustion behavior, as H₂ reacts very differently than natural gas. Traditionally, natural gas has been favored because it is stable, reluctant to ignite, and slow burning, making it a relatively "safe" fuel. This allows engine manufacturers to increase compression ratios with little fear of causing auto-ignition. Hydrogen on the other hand, is relatively easy to ignite and burns quickly.

To describe how prevalent gaseous fuels are to auto-ignition, the Methane Number (MN) scale is used when dealing with natural gas. Similar to the Octane Number scale used with gasoline, the Methane Number is used with natural gas to quantify how easily the fuel will auto-ignite. Methane is used to represent "100 MN", a stable fuel that does not want to auto-ignite. On the low end, H₂ is used to represent "0 MN", a fuel that is likely to auto-ignite. Adding H₂ to the NG fuel will lower the MN of the fuel, and potentially cause some engines to experience end-gas

autoignition (also known as “engine knock”). For this project, the CG137-8 engine used for testing was originally designed to tolerate a wide range of fuel constituents using a relatively low compression ratio, so engine knock was not a concern. Operators with “rich burn” engines that plan on receiving NG fuel blended with H₂ should check that their engines can tolerate the lower MN fuel prior to the change.

Blending H₂ gas with natural gas has been shown to increase the reactivity of the fuel, decreasing ignition delay [13], and increasing flame speed [14]. Zhen et al. found that the increased speed of combustion allowed for more complete oxidation of the fuel, producing less unburned hydrocarbons and CO as more H₂ was used [15]. Dissociation of products is also a common observation with H₂-NG fuel blending, with the generation of NO_x emissions. Akansu et al. observed an increase of NO_x with an increase of H₂, attributing this to the increased flame temperature of the fuel mixture [16]. If H₂ blending increases NO_x and decreases CO production by the engine too much, then there is potential for the 3-way catalyst to malfunction as their proportions change.

Research on this topic has been carried out previously at CSU’s Engines and Energy Conversion Laboratory with collaboration from SoCal Gas. Previous research from 2014/2015 by Prerana Ghotge included H₂-NG fuel blending in a rich burn engine with 3-way catalyst while experimenting with different exhaust gas oxygen (EGO) sensors. Testing for that project was carried out on a 7.5l Cummins-Onan genset while using different EGOs, including a wide band λ sensor (Universal-EGO), and two different narrow band λ sensors (Heated-EGO). Results from that testing showed the best emissions performance from the system operating with the wide band UEGO with up to 20% H₂. The narrow band HEGO were more limited, with the better

sensor tolerating 10% H₂ [17]. Previous research projects at CSU have observed that some narrow band λ sensors can fail due to high NO_x emissions with as little as 5% H₂.

The engine test cell used for the current project is equipped with an advanced engine controller with adaptive response. This is essential when changing the proportions of fuel constituents, as the stoichiometric AFR will change depending on their proportions. Table 1.3.1 shows the expected AFRs of H₂-NG blends, assuming the natural gas to be pure methane (CH₄). As the fuel blend changes, the AFR changes, and the required flow of fuel and air changes. If the engine is operating with a memory-based controller that assumes the fuel, it will surely malfunction as H₂ is added. By controlling the engine with λ in an adaptive closed-feedback loop, the engine will adjust fuel and air flow so that the same proportion of excess air is present in the exhaust, regardless of the changing fuel.

Table 1.3.1. Expected flows of CH₄ and H₂ for CG137-8 engine with a load of 298kW

%H ₂ by vol.	Stoich AFR	Mass flow (kg/hr)					Volumetric flow (l/min)				
		NG (CH ₄)	H ₂	Fuel Mix	Air	Total	NG (CH ₄)	H ₂	Fuel Mix	Air	Total
0%	17.185	66.64	0	66.64	1145	1212	1693	0	1693	16115	17808
5%	17.297	65.53	0.4334	65.96	1141	1207	1665	87.61	1752	16056	17808
10%	17.419	64.34	0.8984	65.24	1137	1202	1635	181.6	1816	15993	17809
15%	17.554	63.07	1.399	64.47	1132	1196	1602	282.7	1885	15924	17809
20%	17.703	61.69	1.938	63.63	1126	1190	1567	391.8	1959	15851	17810
25%	17.869	60.2	2.522	62.72	1121	1184	1529	509.7	2039	15771	17810
30%	18.054	58.58	3.155	61.74	1115	1176	1488	637.8	2126	15685	17811

1.4, Research Objectives

The core objective of this research project is to blend gaseous H₂ fuel with the natural gas fuel supply going to a “rich burn” engine with a 3-way catalyst, and to observe the changes in exhaust chemistry for various concentrations of H₂. Exploration into improving air-fuel controls is an objective as well, with the intention of improving engine emissions. This research project seeks to answer the following questions:

- Will blending H₂ into the NG fuel of a “rich burn” engine with 3-way catalyst cause the engine system to produce high emissions and violate emissions limits?
- Will blending H₂ into the NG fuel of a CG137-8 engine with advanced air-fuel controls cause the engine to malfunction operationally?
- What should engine operators expect with a 20% blend of H₂ (by vol.)?
- What other phenomena should operators be aware of when blending H₂ into their NG fuel supplies, like rapid changes in fuel chemistry?
- How can air-fuel controls be modified to improve catalyst function or to adapt to changing fuel blends?

The following objectives are outlined below to help answer to those questions:

- Blend H₂ into the natural gas fuel of a rich burn engine with 3-way catalyst.
 - o Observe if there is an acceptable limit up to 30% H₂ by vol.
 - o Examine conditions at a 20% blend of H₂ (by vol.), e.g. new λ operating limits.
 - o Explore scenarios with H₂ blending that could cause operators problems in the field.
- Explore air-fuel control improvements.
 - o Verify the improvement from dithering parameters from previous testing.
 - o Explore engine controller parameters, like PID parameter tuning.

This project is taking a testing approach to these objectives, by physically adding H₂ to the fuel stream of an operating engine and observing the changes. Results from this testing are included in Chapters 3 and 4. Chapter 3 includes validation of engine operating parameters, including spark timing, λ operating limits and dithering parameters. Chapter 4 contains all of the results from the H₂ blending tests, including the H₂ concentration sweep, a λ -sweep with a 20%

blend of H₂, and exploration into rapid changes in fuel composition and engine controller response.

CHAPTER 2: METHOD

2.1, Engine Test Cell and Air-Fuel Controls

Testing for this research was conducted on a Caterpillar CG137-8 spark ignited stoichiometric natural gas engine operating with a 3-way catalyst. The CG137-8 is an industrial engine designed to be flexible in fuel constituents, making it ideal for variable fuel testing. An image of this engine test cell is shown in Figure 2.1.1, and some basic information is shown in Table 2.1.1.

Table 2.1.1 (right): Key specifications of the test cell engine and 3-way catalyst.



Engine
Caterpillar CG137-8
400 hp (298 kW) @ 1800 rpm
18 liter, V8, spark ignited
Woodward large engine control module (LECM), electronic fuel regulator (EFR), and throttle
EGO: Bosch 0-258-017-178 narrow band EGO
Catalyst
CAT P/N: 367-5101-05
Volume: 0.076 m ³
Space Velocity: 18,650 hr ⁻¹
Exhaust Flow ~940 m ³ /hr max

Figure 2.1.1 (left): Image of CG137-8 engine test cell at CSU's Powerhouse Engines and Energy Conversion Laboratory.

This engine test cell operates using a cooling water system that services the laboratory with outdoor heat exchangers for cooling. To apply a load to the engine, the driveshaft of the engine is connected to a Dyne Systems eddy current dynamometer (model 1519-3 WIG,

originally made by Eaton Yale and Towns). For all testing in this project the engine was operated at local Northern Colorado air pressure (~84 kPa). However, it is capable of simulating sea-level conditions with an optional pressurized air intake and exhaust flow restriction. All the natural gas fuel used for this project was supplied by the city of Fort Collin's natural gas utility system. Utility natural gas is subject to variability, so the Powerhouse laboratory uses a gas chromatograph to constantly sample the utility natural gas and identify the individual constituents of the fuel.

The CG137-8 engine used for testing was retrofitted with upgraded air-fuel ratio controls from Woodward, including a new electronic fuel regulator, throttle valve, and large engine control module (LECM). This engine came equipped from Caterpillar with compression sensors in each cylinder allowing the control module to measure combustion in every cylinder individually. The LECM was also given full control of individual spark plug ignition timing, utilizing "coil-on-plug" spark plugs. Using combustion data feedback, the LECM can control combustion timing in each cylinder using the Woodward Real Time Combustion and Detonation Control (RTCDC) module. The Woodward LECM together with the RTCDC module are capable of controlling the timing of heat release in each cylinder for every cycle by referencing data from previous combustion cycles.

Natural gas fuel flow is controlled with a Woodward electronic fuel regulator valve prior to mixing with air. The fuel and air are mixed before entering the turbo-compressor. After passing through the turbo-compressor, the fuel-air mixture passes through an electronic throttle and an aftercooler before entering the intake manifold. A schematic representation of the air-fuel system is shown in Figure 2.1.2. Engine speed (rotations per minute, RPMs) is controlled by the LECM using a PID feedback loop referencing a speed sensor on the engine. The LECM controls

engine speed by adjusting the fuel valve and the throttle valve, controlling the flow of the air-fuel mixture into the engine. The load on the engine is measured from the intake manifold pressure, and the LECM is capable of running with different λ setpoints and spark timings depending on the load.

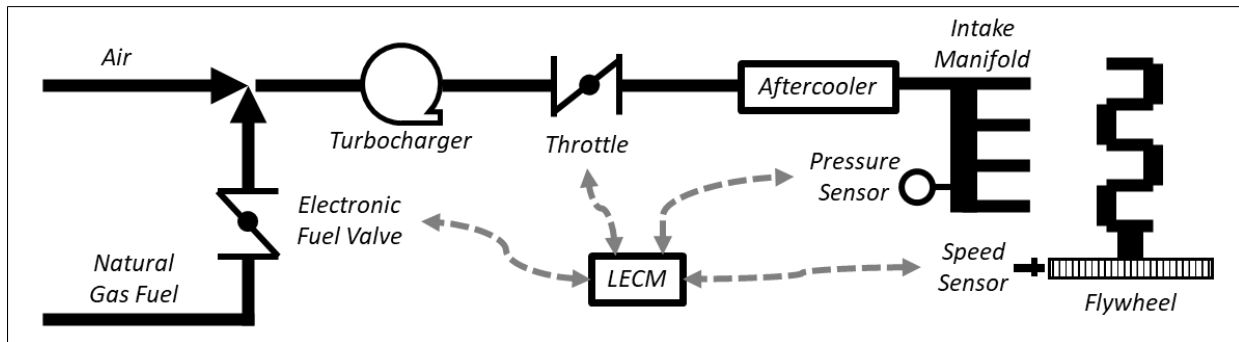


Figure 2.1.2. Schematic representation of the air-fuel supply system on the CG137-8 test cell.

This engine setup is capable of advanced λ control techniques utilizing the Woodward LECM. The ratio of air to fuel in the mixture is controlled by adjusting fuel flow through the electronic fuel valve. λ is measured and controlled by the LECM using a PID feedback loop referencing a Bosch narrow band “rich burn” exhaust gas oxygen (EGO) λ sensor installed on the engine’s exhaust before the 3-way catalyst.

The advanced λ control capabilities on this engine make it much more suitable for changing fuels than classic engines using basic air-fuel ratio controls. In many older engines with basic air-fuel ratio control, fuel flow is assumed based on fuel valve position and fuel pressure, and the resulting λ of the mixture is a calculated value based on assumed fuel flow. In these cases, should the fuel valve become biased or should the fuel composition change, the engine will not be able to recognize the change or adapt to it.

Another capability of this modified engine system is λ -dithering, where λ is fluctuated (dithered) between lean and rich with the intention of improving catalyst conversion efficiency. By dynamically supplying the catalyst with intermittent flows of lean exhaust, replenishing the

catalyst's oxygen storage, the catalyst can theoretically oxidize more carbon-based emissions, improving catalyst performance with a wider range of λ limits. In previous testing at CSU in 2020, λ -dithering techniques were explored on this same CG137-8 engine setup to improve catalyst conversion efficiency. Results indicated that a λ -dithering frequency of 1.5% amplitude at 1 Hz was effective at improving catalyst function, and those parameters were used during this research. An example of λ -dithering is shown in Figure 2.1.3.

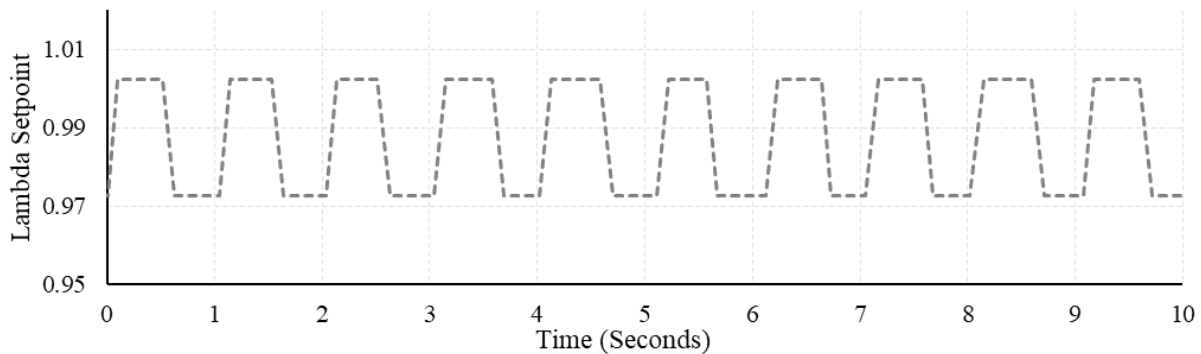


Figure 2.1.3. An example of λ -dithering collected from the CG137-8 engine system.

When testing, engine setpoint parameters and operating conditions must be continuously collected. Most data concerning the LECM (like λ or spark timing) are collected by a Woodward Toolkit program in communication with the LECM via a CAN bus. Combustion data is collected by the RTCDC module directly. All other data collection, like temperatures, dynamometer feedback, and emissions analyzer data are collected using a LabVIEW program utilizing a NI CompactRIO DAQ system that services the laboratory. Examples of data collected and screenshots of the user interfaces can be found in Appendix A.

2.2, Three-Way Catalyst and Emissions Sampling

Analyzing emissions before and after the catalyst gives us the ability to assess engine and catalyst performance individually. Exhaust emissions from the engine can be sampled pre-

and post-catalyst via a heated sample line with a remote emissions analyzer located elsewhere in the lab. The laboratory is equipped with Siemens emissions analyzers measuring carbon monoxide (CO), carbon dioxide (CO₂), nitrogen oxides (NO_x), oxygen, and unburned hydrocarbons (THCs). The lab is also equipped with a Fourier transform infrared (FTIR) spectrometer allowing for measurements of volatile organic compounds (VOCs), hydrocarbon speciation, formaldehyde, acrolein, acetaldehyde, and ammonia. The emissions analyzers used for this project are shown in table 2.2.1. The natural gas fuel constituents were measured using an Inficon MicroGC.

Table 2.2.1. Emissions analyzers used with this project.

Instrument	Species Analyzed
Siemens NOXMAT 600	NO _x
Siemens OXYMAT 6	O ₂
Siemens ULTRAMAT 6	CO and CO ₂
Siemens FIDAMAT 6	Total Unburned Hydrocarbons
MKS Multigas FTIR	VOCs, HC Speciation, CH ₂ O, NH ₃ , Acrolein, and Acetaldehyde

In preparation for the current project, a new 3-way catalyst was chosen and installed on the engine. Emissions goals for this testing were set at 0.15g/bhp-hr and 0.6g/bhp-hr for NO_x and CO, respectively. This decision was made with input from representatives at Southern California Gas, who referred to the current Best Available Control Technology (BACT) requirements [18], and also with advice from Caterpillar engineers.

An inline NO_x sensor (made by ECM) is also located directly on the engine exhaust, post-catalyst. This sensor provides live feedback to the LECM via a CAN on post-catalyst NO_x emissions. The inline exhaust NO_x sensor is good to reference when considering the timing of chemical changes in the catalyst and exhaust, and the remote analyzer is more accurate when

measuring total quantities of chemical emissions. A comparison between the inline NO_x sensor and the remote Siemens chemiluminescence NO_x analyzer is shown below in Figure 2.2.1.

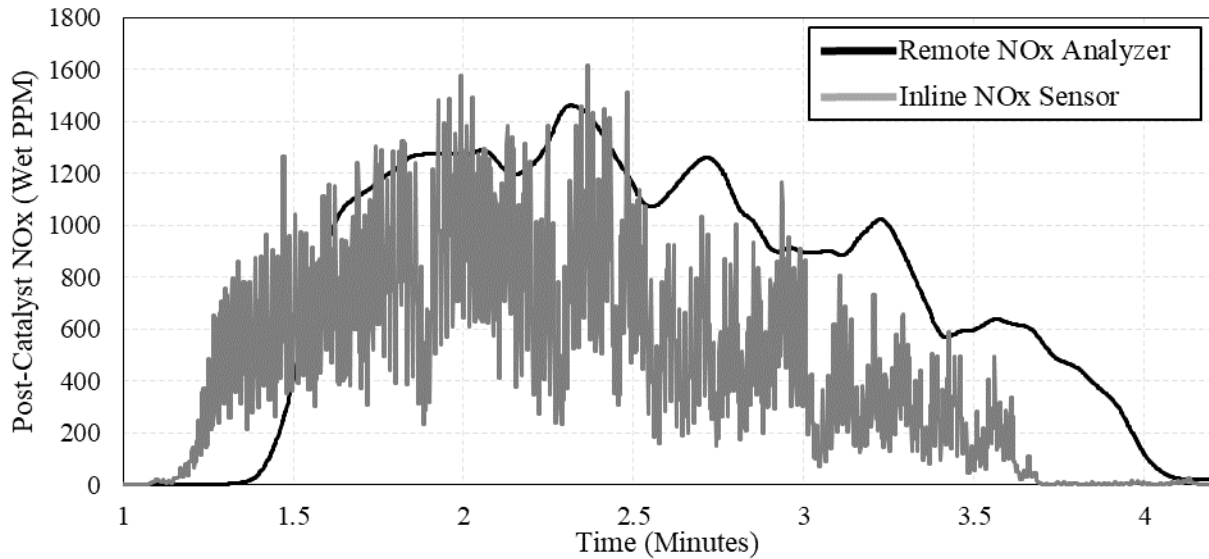


Figure 2.2.1. A comparison between the inline NO_x sensor and remote NO_x analyzer as NO_x emissions change in post-catalyst exhaust.

2.3, Fuel Blending

A H₂ distribution system was designed to connect with a large H₂ storage trailer and deliver compressed H₂ gas to the engine within the lab. To make precise fuel blends, a mass-flow meter/controller using differential pressure-based laminar flow measurement was installed on the H₂ fuel supply (Alicat, model:MCR-500SLPM-D-67X86). A Coriolis mass-flow meter previously installed on the natural gas fuel line was utilized to measure NG flow. A feedback control loop was written in a LabVIEW program to monitor the flow of natural gas through the Coriolis meter and adjust H₂ flow to meet the required proportions. The H₂ and NG are blended before the LECM controlled fuel valve (Woodward, model:8407-803), and the LECM is given no warning of fuel changes in this test setup. A basic schematic of the air-fuel system is shown in Figure 2.3.1, and a screenshot of the H₂ control system in LabVIEW is shown in figure 2.3.2.

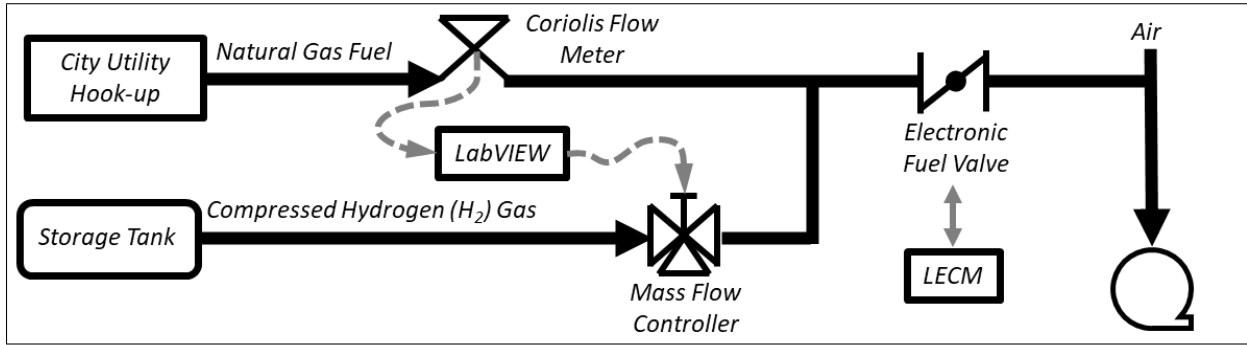


Figure 2.3.1. A basic schematic of the H₂-NG fuel blending system. Fuel flow proportions are based on the natural gas flow, and the engine controller is unaware of fuel changes.

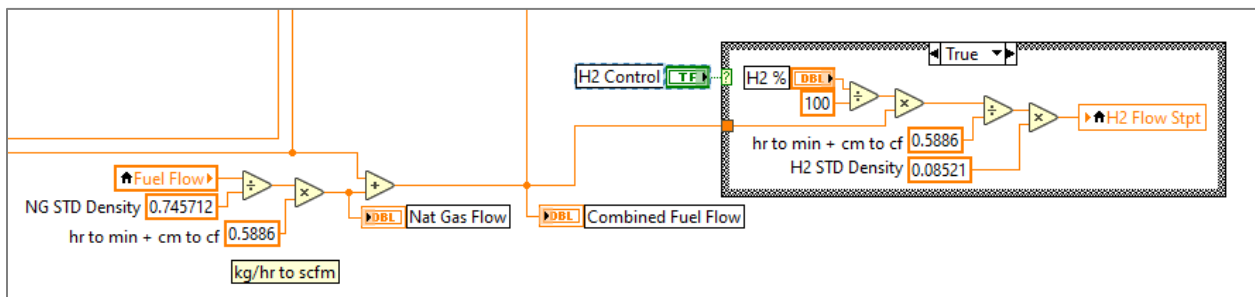


Figure 2.3.2. Screenshot of the H₂ control loop in LabVIEW that controls the flow of H₂ proportionally to the flow of natural gas.

This fuel blending system was designed to change the composition of the fuel abruptly to evaluate engine controller response. This system is representative of engines that are operating on natural gas utilities that will receive H₂ blended fuel. Additional schematics and descriptions of the H₂ blending system at the Powerhouse laboratory can be found in Appendix B.

When H₂ is added the fuel volumetric flowrate increases. H₂ is less energy dense than natural gas by volume, so the engine intake and auxiliary equipment must be large enough to accommodate the increased volumetric fuel flow. Expected volumetric fuel and air flows for the engine are shown below in Table 2.3.1, showing increased fuel mix flow. At a 20% blend of H₂ - fuel flow must increase by 15% to maintain the same energy delivery rate.

Table 2.3.1. Expected flow rates for CG137-8 engine with a load of 298kW

%H ₂ by vol.	Stoich AFR	Volumetric flow (l/min)				
		NG (CH ₄)	H ₂	Fuel Mix	Air	Total
0%	17.185	1693	0	1693	16115	17808
5%	17.297	1665	87.61	1752	16056	17808
10%	17.419	1635	181.6	1816	15993	17809
15%	17.554	1602	282.7	1885	15924	17809
20%	17.703	1567	391.8	1959	15851	17810
25%	17.869	1529	509.7	2039	15771	17810
30%	18.054	1488	637.8	2126	15685	17811

2.4, Testing Procedure

All data collection for this research was recorded from the engine while it was running in “steady state”. Using an eddy current dynamometer (Dyne Systems model 1519-3 WIG), a constant load of 1580Nm was applied to the engine while it held a constant 1800rpm, resulting in a constant maximum power output of 298kW.

While collecting data for different H₂ fuel concentrations, the engine system was given time to settle after changing fuel blends. For each data point the engine was given time to stabilize, often for up to 30 minutes to be sure that valid data was collected. An example of a fuel transition is shown in Figure 2.4.1, where H₂ was increased from 10% to 15%. In Figure 2.4.1, the engine was operating with a dithering λ , so feedback from the EGO sensor oscillates and can be difficult to interpret. To make λ easier to visualize, the plot shows an average λ where 3-second moving averages were applied to the EGO sensor feedback.

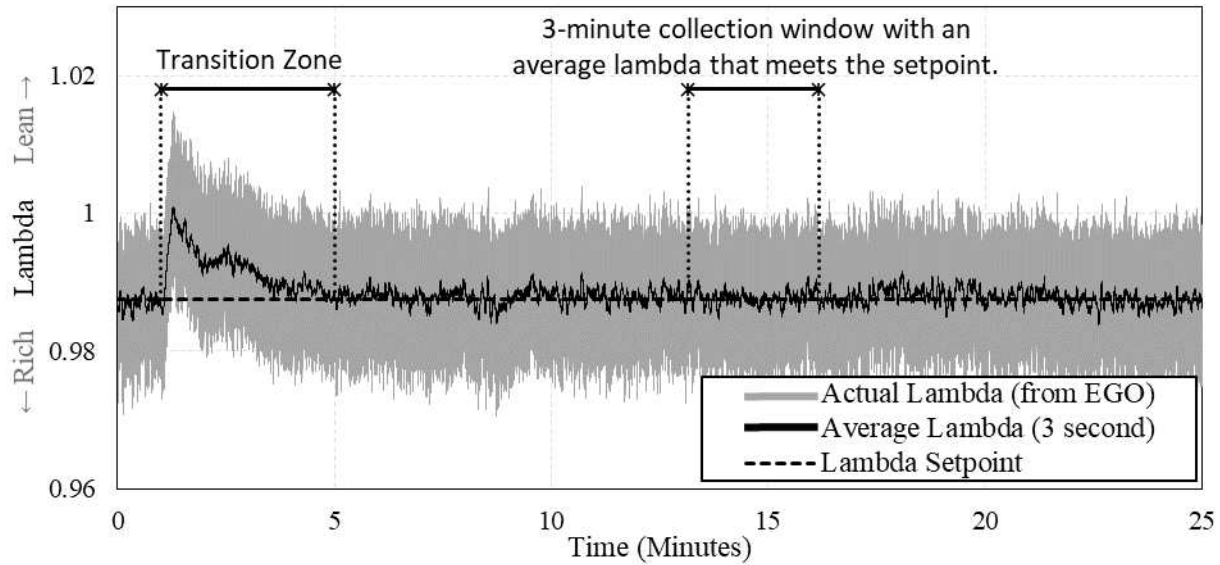


Figure 2.4.1. An example plot of λ vs. time after increasing H_2 from 10% to 15%.

Careful attention was paid to make sure that the average λ for each collection point was the same. This was important to limit the influence of λ on exhaust products, as λ can have a much more profound effect on emissions than fuel blends. While processing the collected data, 3-minute window averages were selected where the engine was operating with little changes and the average λ value was the same as the setpoint. As an example, Figure 2.4.1 shows the 3-minute collection window used for the 15% H_2 data point. All subsequent data like emissions or fuel flows were then averaged from the same 3-minute time window.

An overview of the testing carried out on the CG137-8 is shown below in Table 2.4.1. The first testing was a spark timing sweep to choose a constant ignition timing to maintain throughout testing. Next, was a natural gas baseline λ -sweep, to outline the window of operation where the 3-way catalyst was most effective. This baseline sweep was carried out with a steady λ and a dithering λ to compare catalyst behavior with different λ controls. Using data from the λ -sweep, the window of operation was defined, and the midpoint of the window was chosen to be

the constant λ value for the H₂ blending sweeps. After the baseline sweeps, dithering parameters were also explored, in response to results from the baseline sweeps.

Table 2.4.1. List of testing carried out on the CG137-8 engine test cell.

Test	Exhaust Sampling	AFR control	Section
Spark timing sweep	Post-cat	Steady	3.1
Baseline λ sweep	Pre- and Post-Catalyst	Steady	3.2
Baseline λ sweep	Pre- and Post-Catalyst	Dither	3.2
Exploring dithering parameters	Post-cat	Dither	3.3
H ₂ % sweep	Pre- and Post-Catalyst	Steady	4.1 & 4.3
H ₂ % sweep	Pre- and Post-Catalyst	Dither	4.1 & 4.3
λ sweep with 20% H ₂	Pre- and Post-Catalyst	Dither	4.2
PID tuning with H ₂ transitions	Post-cat	Dither	4.4

Once operating parameters for the engine were selected, H₂ blending began. While holding λ constant, H₂ was introduced into the natural gas fuel in 5% increments up to 30% by volume. For each concentration of H₂, all operating parameters were held constant for up to 30 minutes to ensure λ had returned to the setpoint, and to reduce the possibility of hysteresis in the catalyst from previous datapoints. After the H₂ sweeps, a λ sweep was conducted similar to the baseline, but with a 20% blend of H₂ by volume. Finally, PID tuning was carried out on the engine while transitioning H₂ concentrations, to improve engine controller response.

CHAPTER 3: BASELINE TESTING AND OPERATION PARAMETER ANALYSIS

3.1, Spark Timing Exploration

One of the first parameters to determine for testing was spark timing. The CG137-8 engine utilizes coil-on-plug assemblies so that the LECM can control the timing of each spark plug individually. The timing of spark ignition should be precise, as changing spark timing can have a dramatic effect on combustion behavior in the cylinder and on the products of combustion in the exhaust. Most traditional engines operate with constant spark timing, using the same spark timing for every cylinder for a given engine, and are only changed when tuning the engine. Newer engines that come with advanced engine controllers are often capable of adapting the spark timing with changing conditions while the engine is running. Adaptive spark timing is a very beneficial capability for modern engines, allowing the engine to adapt to changing conditions and control heat-release to the correct timing.

For most of this testing, we chose to use constant spark timing. This decision was made to make this testing more comparable to most engines operating in the field. To choose an ideal spark timing, a spark timing sweep was first conducted. For this sweep, the engine was held at a constant λ value near the middle of the λ -compliance window, and the spark timing was swept from 20° to 35° BTDC (crank angle degrees Before Top Dead Center) for all cylinders. The results from the timing sweep are shown in Figure 3.1.1. After examining the results from the spark timing sweep, we chose 27° BTDC as the constant spark timing to use during testing because it resulted in good efficiency with high peak pressure and low fuel consumption.

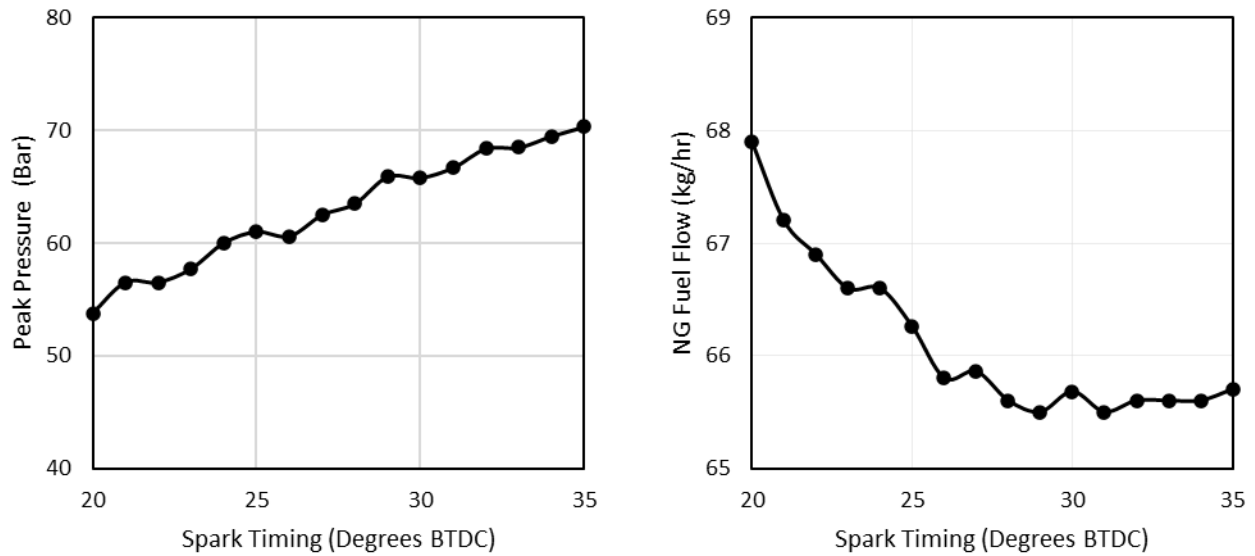


Figure 3.1.1. Results from the spark timing sweep, with peak pressure shown on the left, and fuel flow shown on the right.

3.2, Baseline λ -Sweep

The next parameter to determine before testing was the λ setpoint value for the engine to use throughout testing. As discussed previously in Section 1.2.1, the λ that the engine operates with determines the products of combustion in the exhaust, and subsequently the performance of the catalyst in reducing the targeted emissions. Every fuel type has a specific proportion of air required, depending on the chemical composition of the fuel. As the chemical proportions of a fuel change, so should the stoichiometric ratio of air to fuel. To account for this, λ is the chosen parameter to control their proportions, as λ will maintain the intended stoichiometric ratio of air to fuel using feedback from the λ sensor in the exhaust.

The procedure to choose a constant λ value for testing started with a λ -sweep, to find the window that the engine can operate within while staying below the emissions goals for NO_x and CO. Results from this baseline λ -sweep are shown in Figure 3.2.1, and the effect of the catalyst on exhaust emissions can be seen by comparing pre- and post-catalyst emissions.

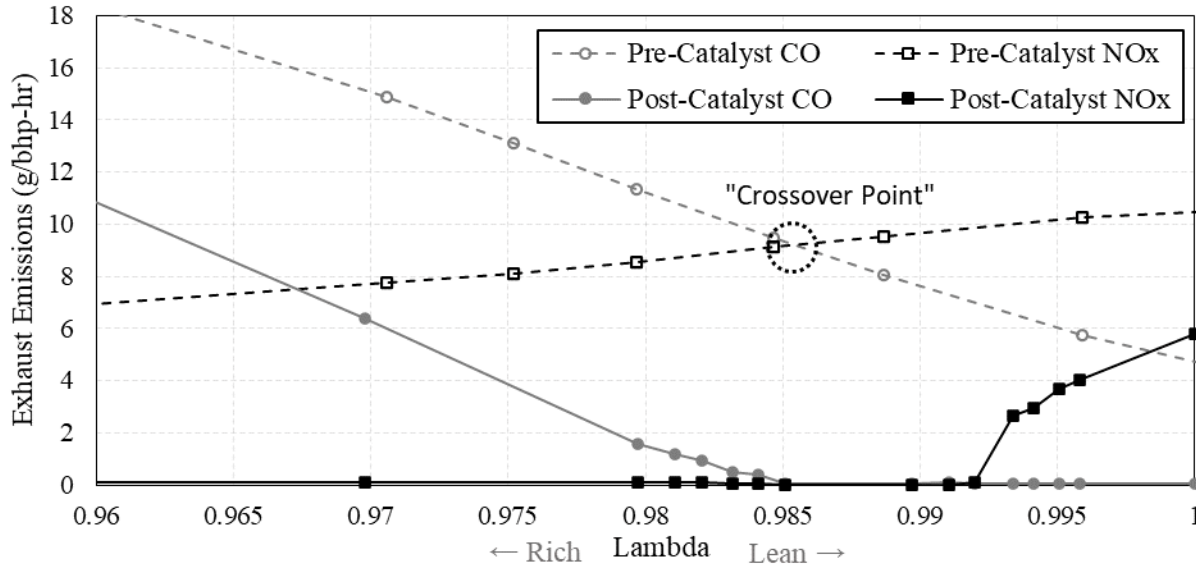


Figure 3.2.1. Pre- and post-catalyst NOx and CO emissions comparison from natural gas baseline λ -sweep test.

Pre-catalyst NOx and CO trend on straight lines, but post-catalyst emissions are irregular because the effectiveness of the catalyst depends on the proportion of pre-catalyst NOx and CO. Catalyst conversion efficiency is calculated to assess the effectiveness of the catalyst. This is accomplished by finding the individual percentages of CO and NOx reduced in the catalyst, and then only considering the minimum values of the two percentages. Catalyst conversion efficiency can be seen in Figure 3.2.2. When the engine is operating too rich there is not enough reagent to oxidize all the CO, resulting in a gradual increase in post-catalyst CO. When the engine is operating too lean, the catalyst becomes saturated with excess oxygen and cannot reduce NOx, resulting in a sharp increase in post-catalyst NOx production.

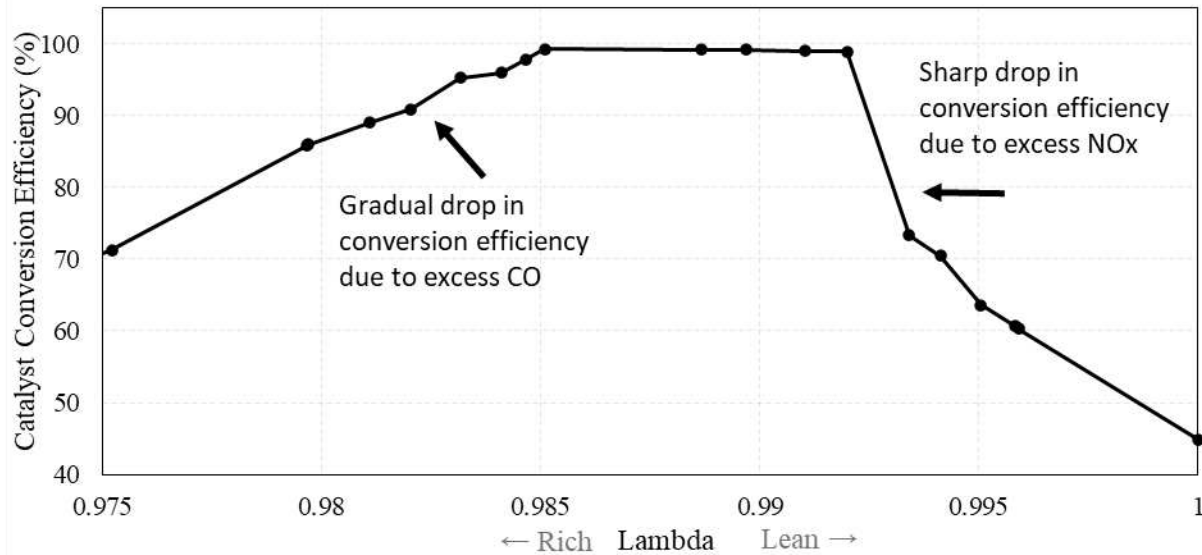


Figure 3.2.2. Catalyst Conversion Efficiency, considering the percentage of NOx and CO eliminated in the catalyst.

Using the data from the baseline λ -sweep, boundaries for the window of operation were established where post-catalyst NOx and CO exceeded our goals of 0.15g/hp-hr and 0.6 g/hp-hr respectively. These limits are shown in Figure 3.2.3, and the engine must operate between these two λ values to stay below our desired emissions limits. The region between these two λ values is often called a “window of compliance” or “window of operation”. Straying from this window typically results in high emissions of CO if too rich, or NOx if too lean.

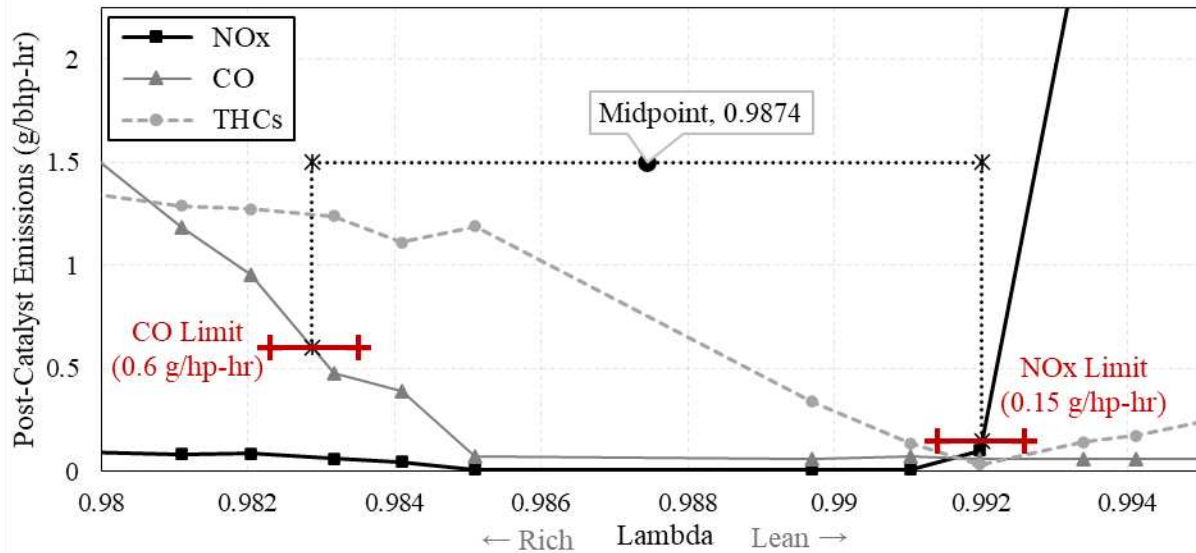


Figure 3.2.3. Post catalyst NOx, CO, and THC emissions from natural gas baseline λ -sweep test with more detail, showing the rich and lean limits used to find the window of operation.

For this project, a constant λ value had to be chosen to use while experimenting with H₂. Using a constant λ setpoint is important because changes in λ will likely have a larger effect on exhaust constituents than changes in the fuel. We chose to use the midpoint of the window of operation because this results in the largest margin for error in λ control. The best λ point to operate at is near the lean-limit because THCs are at their minimum and CO/NOx are below emissions limits. However, this is not a very stable point for the catalyst, as catalyst conversion efficiency drops off fast if the engine λ value drifts lean.

Additionally, the window of operation for “stoichiometric” engines is actually slightly rich of stoichiometric ($\lambda=1$ for a stoichiometric air-fuel ratio), giving merit to their name as “rich burn” engines. This also correlates with the “crossover point”, which can be seen in Figure 3.2.1. The window of operation often occurs near the λ value where NOx and CO mass flows are the same entering the catalyst.

3.3, Dithering Technique

The next parameter to finalize before testing was λ -dithering frequency and amplitude. Prior testing on dithering has been conducted on the same CG137-8 engine at the Powerhouse Lab during 2020 by Andrew Jones [12]. Results from their testing indicated that a dithering fluctuation of 1.5% of the λ value at a frequency of 1 Hz was ideal to improve catalyst conversion efficiency. A sample of data representing dithering behavior in the engine is shown below in Figure 3.3.1. This sample shows the λ setpoint, fuel valve position, the delay in feedback from the EGO sensor, and the resulting post-catalyst NO_x emissions. The engine was operating lean at the time of this sample window. With the engine operating lean, the catalyst was saturated with oxygen, resulting in NO_x production that matched λ from dithering cycle to dithering cycle.

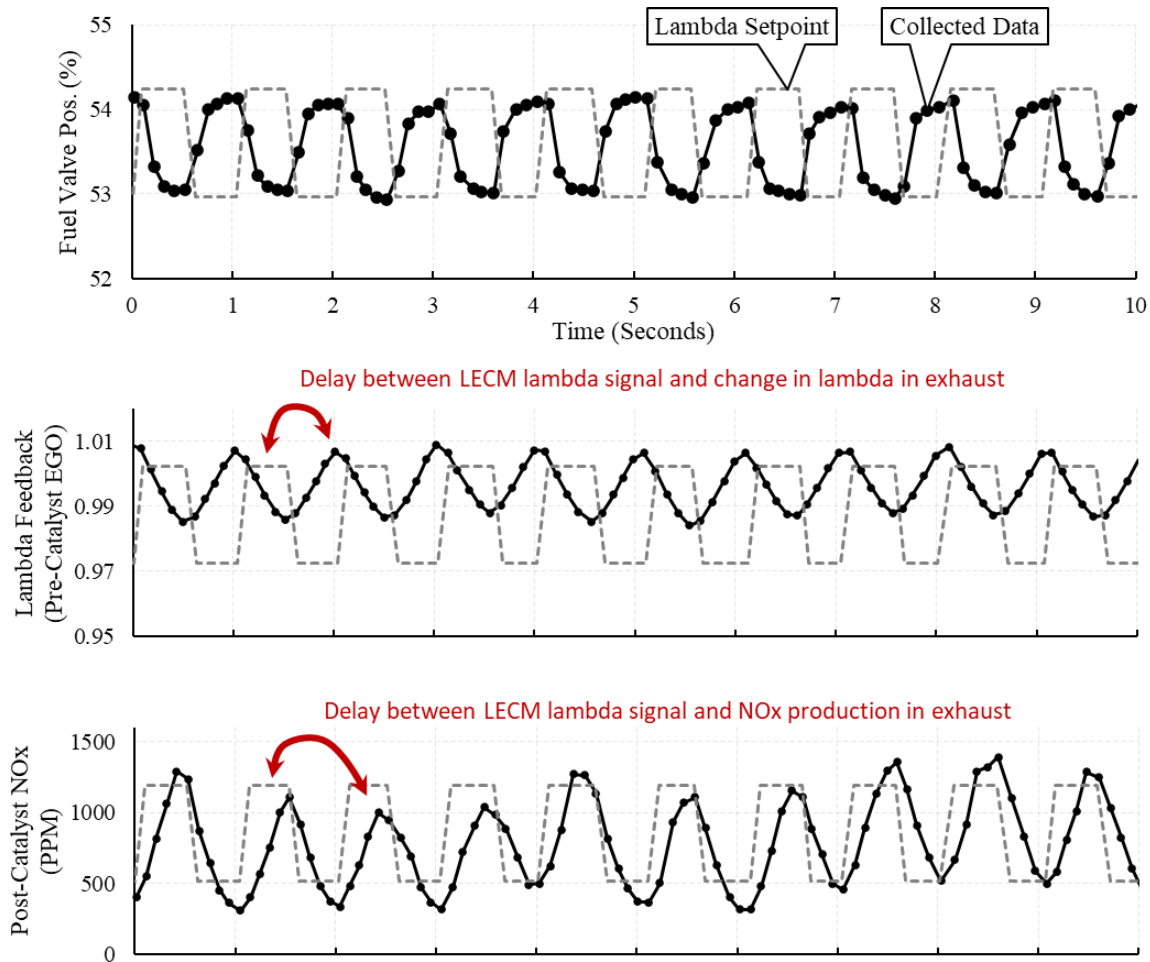


Figure 3.3.1. Sample data showing dithering, where the λ setpoint precedes the change in λ feedback in the exhaust and produces proportional NOx in the exhaust.

It was decided that we should verify these parameters for the current project, as a new 3-way catalyst had been purchased and new emissions goals had been chosen. Two baseline λ -sweeps were conducted, one with steady λ control and the other with dithering λ control set at 1.5% amplitude and at 1Hz. The initial results from these baseline sweeps indicated that dithering had a negative effect on catalyst performance, and narrowed the engine's λ -window of operation. Results comparing the steady and dithering λ -sweeps are shown in Figure 3.3.2.

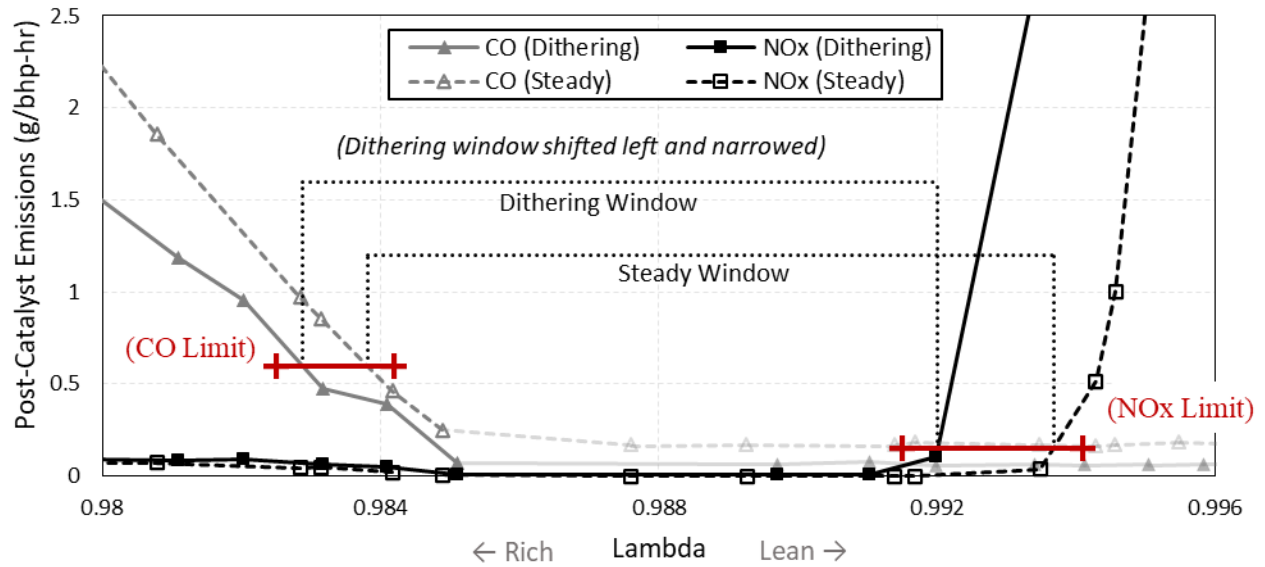


Figure 3.3.2. Comparison between steady and dithering λ -sweeps, showing that the window of operation shifted to the rich-side and narrowed slightly.

Dithering is intended to improve catalyst performance, so having the window of operation narrowed while dithering was not ideal. Some exploratory testing was then conducted to identify better operating parameters. Multiple frequency sweeps were conducted while holding the amplitude constant, testing 1%, 1.5%, and 2% amplitude at 3 different λ -values, lean, center, and rich. One of the frequency sweeps for 2% amplitude is shown in Figure 3.3.3.

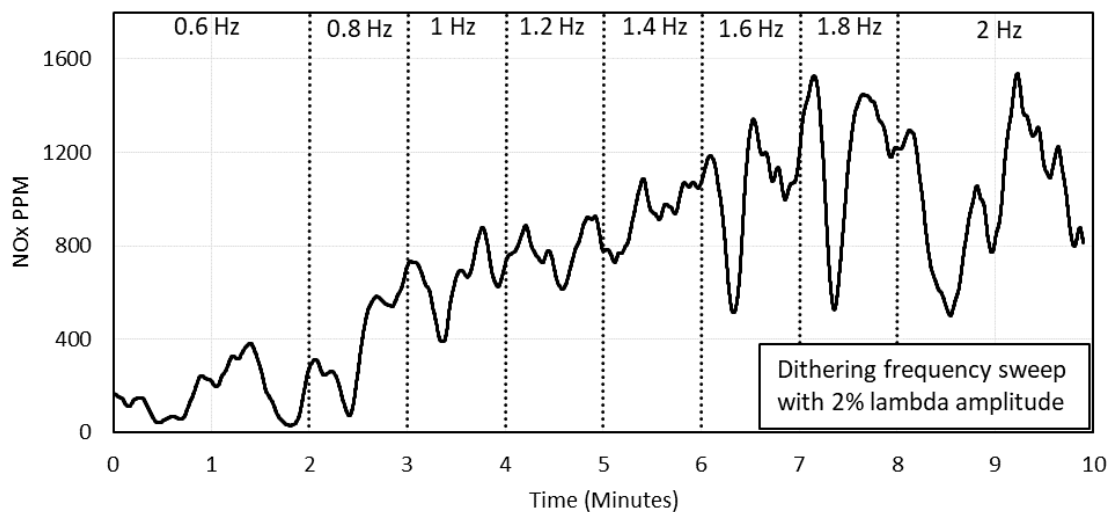


Figure 3.3.3. Dithering frequency sweep with 2% λ -amplitude at a lean setpoint. Since this sample was operating at a lean setpoint, reducing NOx production was the intention.

Results from these frequency sweeps were inconclusive, and further testing is advised. In future testing, lower frequencies should be explored, as the lowest tested in this project was 0.6 Hz. Results from Defoort et al. state that a 5-second period (0.2Hz) was most effective for their catalyst [11]. Additionally, future dithering testing on natural gas engines should include biased waveforms. The time the engine operates lean should match the amount of time it takes for the catalyst to become saturated with oxygen, and the time the engine operates rich should match the amount of time it takes for the catalyst to deplete its oxygen storage.

To support H₂ blend testing, we decided to continue using the operating parameters found in previous testing of 1.5% amplitude at 1Hz, even though they did not show an improvement in catalyst performance. This decision was made with the intention of making λ fluctuations more predictable. Even while the engine is operating with a steady λ signal, λ continues to fluctuate as engines running “steady” are never truly steady. A comparison between steady and dithering operation is shown below in Figure 3.3.4. By using a dithering λ control, fluctuations in λ are periodic and can be repeated through different tests.

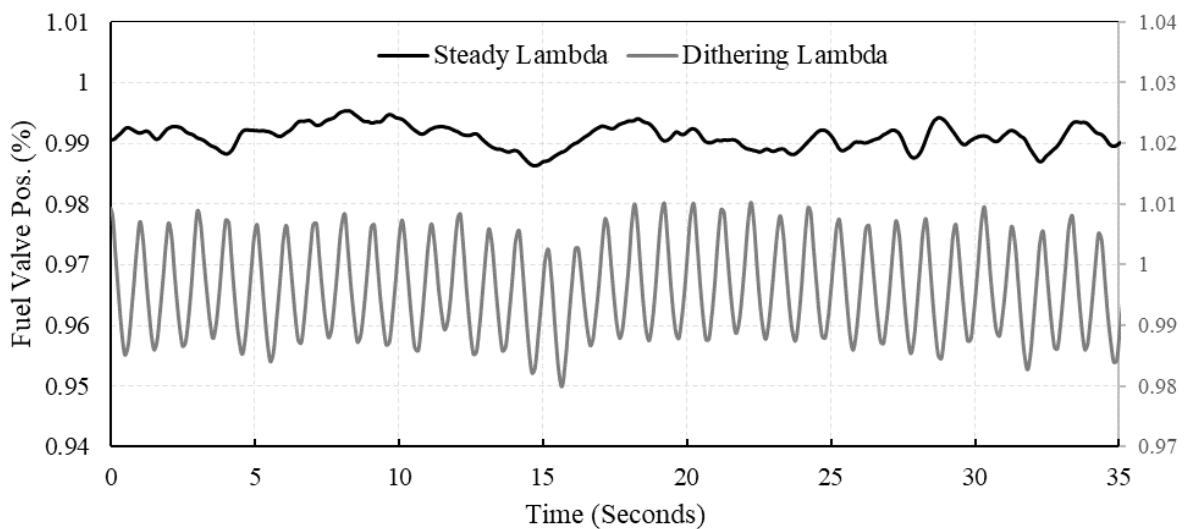


Figure 3.3.4. Comparison between steady and dithering operation, showing that steady operation is not truly steady while dithering fluctuations are periodic.

CHAPTER 4: HYDROGEN FUEL BLENDING

4.1, Hydrogen Fuel Concentration Sweep

Blending hydrogen with natural gas changed the combustion behavior of the fuel, causing the fuel to ignite faster and increase peak pressure. The change in ignition delay and peak pressure location are shown in Figure 4.1.1. Estimating ignition delay as the crank angle degrees between the ignition spark and 10% heat release, ignition delay was shortened by ~6% at 20% H₂. This is in line with Gersen et al., who found that increased levels of H₂ blended with methane decreased the ignition delay of the fuel, showing increased reactivity [13]. Additionally, cylinder peak pressure increased with increasing H₂, shown in Figure 4.1.2. This is also a recognized combustion behavior with H₂ addition, which Karim et al. attributes to faster reaction initiation and propagation [19].

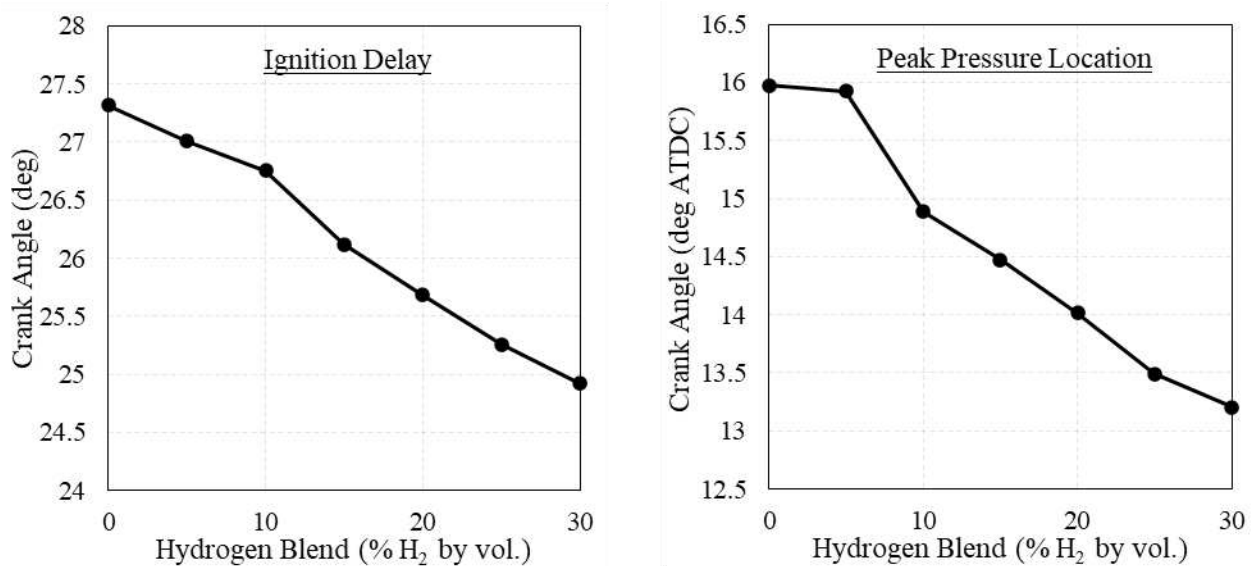


Figure 4.1.1. Ignition delay and peak pressure location with increasing H₂.

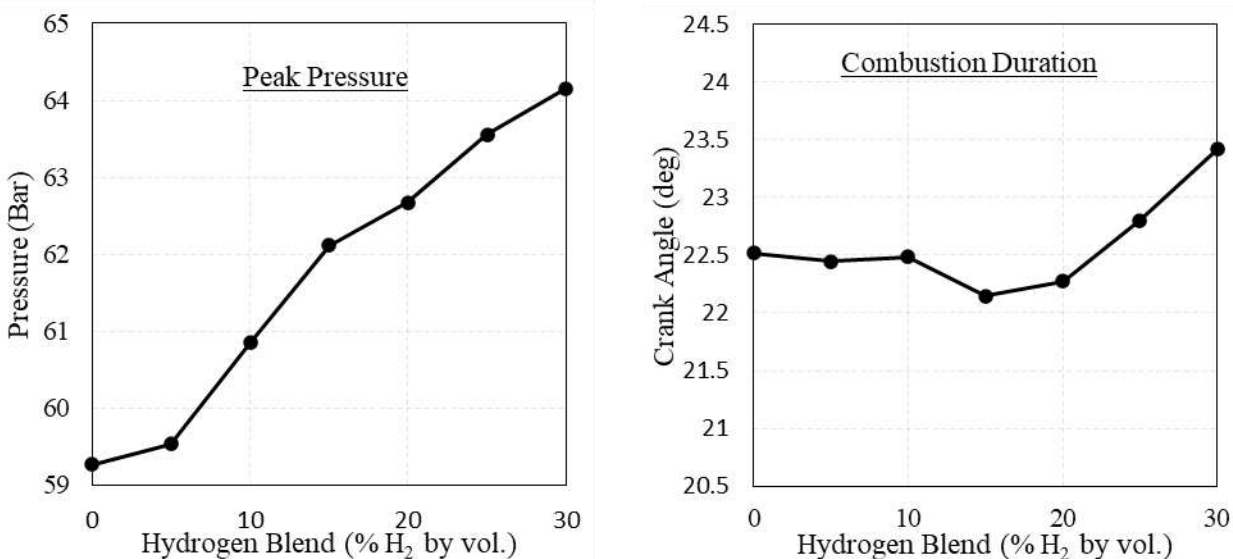


Figure 4.1.2. Cylinder peak pressure and combustion duration with increasing H₂.

Pre- and post- catalyst NO_x and CO emissions are shown below in Figure 4.1.3. Pre-catalyst NO_x and CO emissions behaved as expected. With increased H₂ - CO decreased and NO_x increased. The decrease in CO is described by Xudong et al. as they attribute the reduction in CO to be caused by more complete oxidation of the hydrocarbons [20]. The increase in NO_x is explained by Akansu et al. as a result of increased flame temperature caused by the increasing H₂ content [16]. Post-catalyst emissions did not respond as expected though, with insignificant changes to both CO and NO_x. We attribute this to the fact that the catalyst was still performing well and operating near the center of its λ -window of compliance.

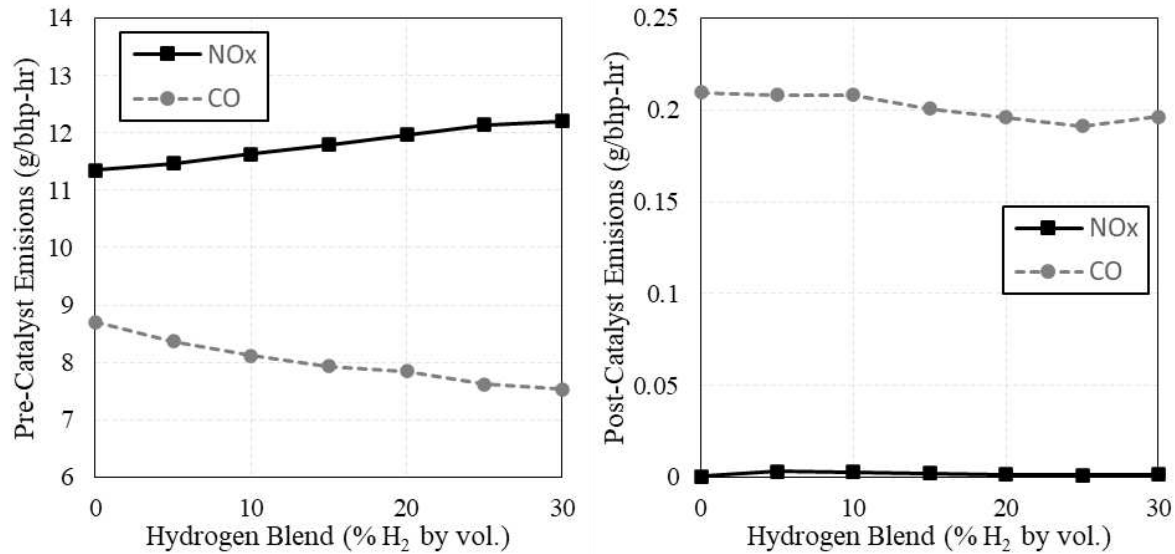


Figure 4.1.3. *NO_x and CO emissions vs. H₂ fuel concentration, pre-catalyst emissions shown on the left, and post-catalyst emissions shown on the right.*

The initial H₂ blending sweep indicated that the engine and catalyst can tolerate elevated levels of H₂ as long as the engine is able to maintain the optimal λ setpoint. Post-catalyst emissions before blending H₂ was already very low, so the effect of H₂ on CO and NO_x emissions was minimal. These results show that this engine system can tolerate up to at least 30% H₂ without exceeding CO and NO_x emissions limits. This conflicts with previous testing on this subject at CSU from 2014/2015, where they found the system could not exceed 10% H₂ while operating with a narrow band EGO [17]. This discrepancy is likely because the previous project used a tighter NO_x limit of 11ppmd (appx. 0.04g/hp-hr). Also, the current project is using advanced λ control software and equipment, maintaining λ with feedback loops instead of assuming air-fuel ratios.

Brake thermal efficiency is shown below in Figure 4.1.4, displaying slight increases in efficiency above 10% H₂. Also shown in Figure 4.1.4 is the change in total fuel mass flow compared to the lower heating value of the mixture. As NG is replaced with H₂ in the fuel, the heating value of the fuel mixture increases, requiring less fuel to maintain speed and load.

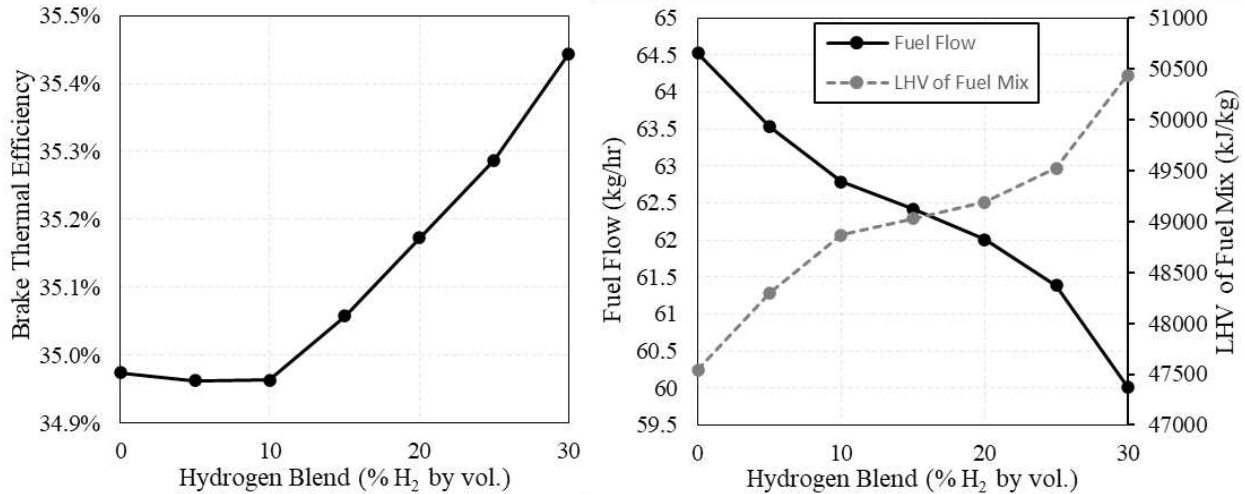


Figure 4.1.4. Brake thermal efficiency shown on the left, and total fuel mass flow compared with the LHV of the mixture on the right.

The core objective for H₂ blending is to reduce greenhouse gas (GHG) emissions from combustion. This expectation was validated by the current testing. At 20% H₂ in the fuel – natural gas flow was reduced by 7.3% causing a 7.1% reduction of CO₂ in the post-catalyst exhaust. The change in fuel flows and CO₂ emissions are shown below in Figure 4.1.5.

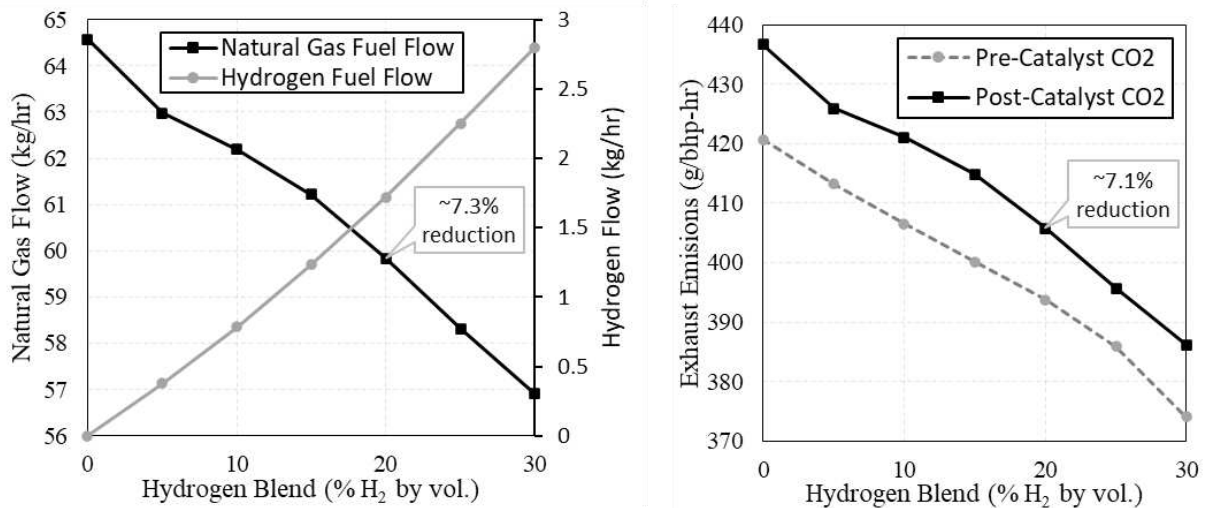


Figure 4.1.5. Changing fuel flows and CO₂ emissions with increasing H₂.

An unexpected benefit from H₂ blending was a reduction in total hydrocarbons (THCs) and methane (CH₄) in both the pre- and post-catalyst exhaust, shown below in Figure 4.1.6. This

is likely caused by better combustion initiation due to the elevated levels of H₂. Methane is now recognized as a greenhouse gas (GHG) contributor, so lowering post-catalyst methane emissions should also be considered when evaluating the change in GHG emissions with increasing H₂. Referencing the EPA’s GHG evaluation of methane, methane emissions are multiplied by a weighted factor of 25 when comparing methane and CO₂ [21], and these two values can be added together to find CO₂-effective (CO₂-e). At a blend of 20% H₂ - post-catalyst GHG emissions (CO₂-e) were reduced by 8.1%.

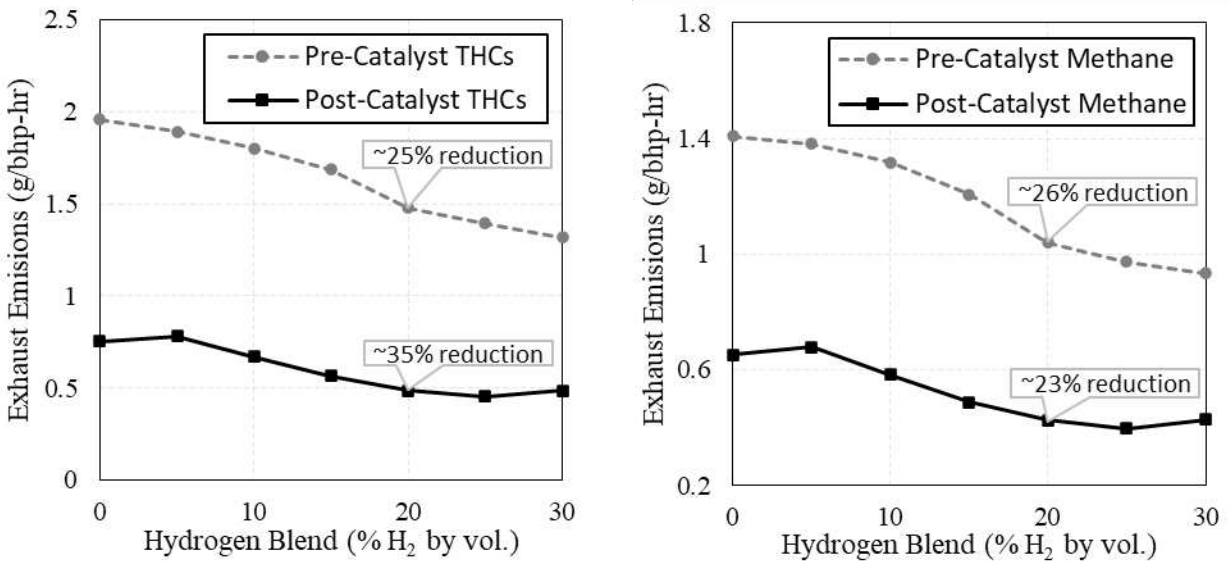


Figure 4.1.6. Emissions of hydrocarbons (THCs) and methane with increasing H₂.

Additionally, levels of volatile organic compounds (VOCs) and formaldehyde in the exhaust were also measured during testing. Shown in Figure 4.1.7, both VOCs and formaldehyde decrease pre-catalyst as H₂ is increased, with formaldehyde showing a linear trend. Post-catalyst, there is very little change because emissions were already so small.

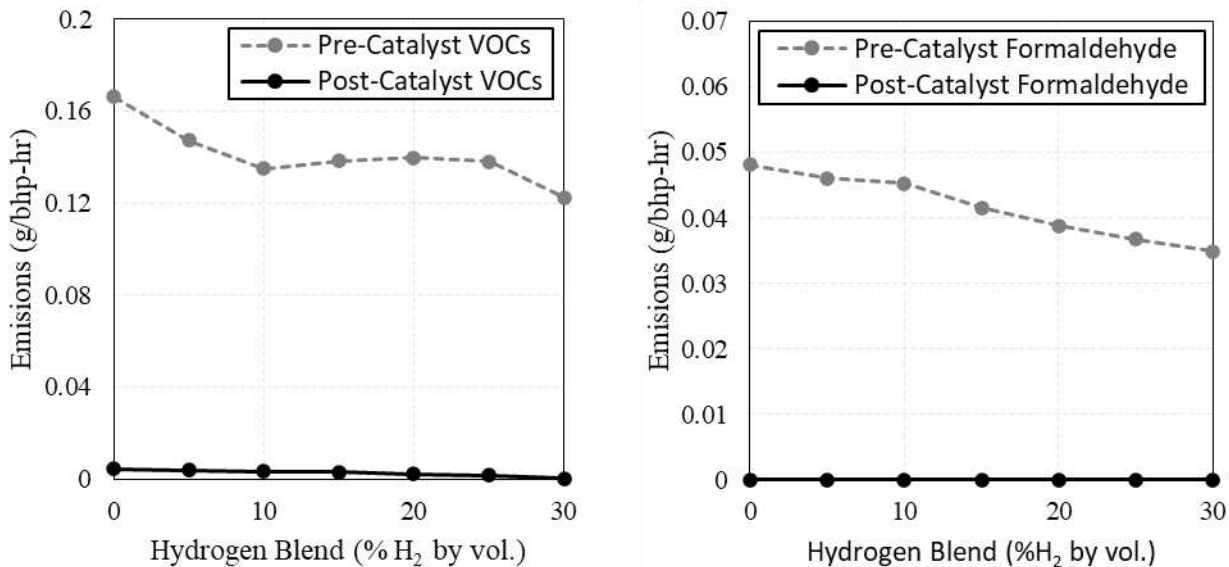


Figure 4.1.7. Emissions of volatile organic compounds (VOCs) and formaldehyde (CH_2O) with increasing H_2 .

Finally, Post-catalyst ammonia also showed a clear reduction, indicating less ammonia generation in the catalyst. Ammonia is generated in the catalyst when the exhaust is oxygen deficient and there is excess H present, usually happening when the engine is running rich [11]. With the addition of H_2 into the fuel, we expected a possible increase in post-catalyst ammonia due to the increased H in the fuel, however the opposite was observed. Shown in Figure 4.1.8, at a 20% blend of H_2 – ammonia generation was reduced by 55%.

Additionally, while ammonia is decreasing, catalyst exhaust temperature is also decreasing. Catalyst operating temperature is regulated by the EPA, to ensure proper ammonia reduction. Results from this testing indicate that at elevated levels of H_2 in the fuel, the catalyst may be able to operate at lower temperatures with little ammonia generation.

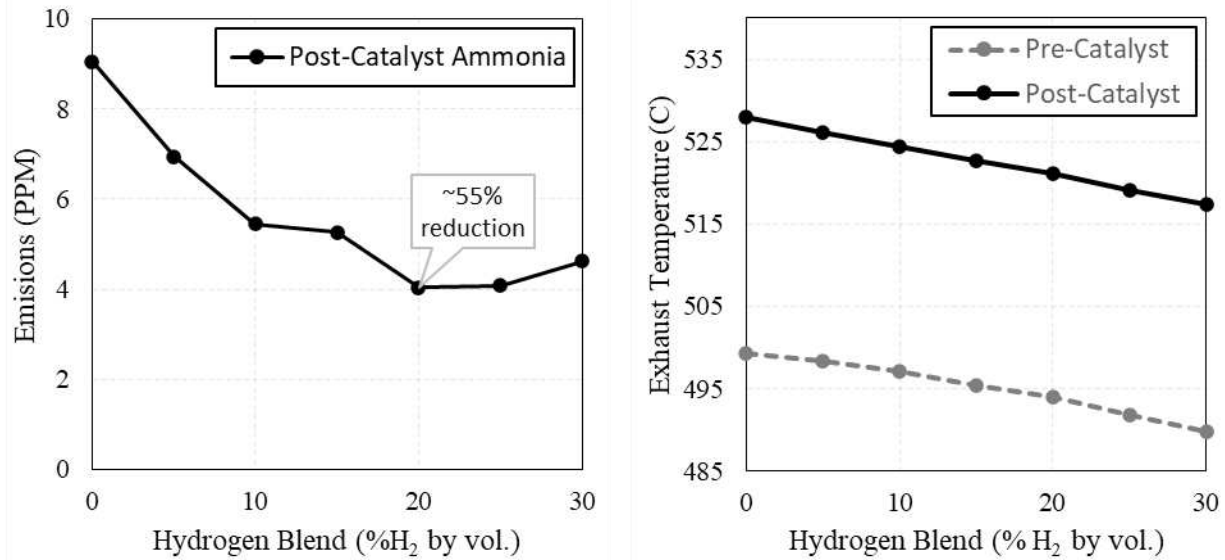


Figure 4.1.8. Post-catalyst ammonia emissions and exhaust temperatures with increasing H₂.

While post-catalyst ammonia emissions decrease as H₂ is increased up to 20%, at levels beyond 20% H₂ - ammonia looks like it could be increasing again. This could be an indication that as H₂ continues to increase, ammonia may also continue to increase as more H finds its way to the catalyst. Further testing is advised to measure ammonia generation in the catalyst at elevated levels of H₂ beyond 30%.

4.2, λ-Sweep with 20% H₂ Blend

The effect of reducing NO_x (post-catalyst) with added H₂ indicated that H₂ blending impacted more than just in-cylinder combustion. To investigate further, a λ-sweep was conducted with a blend of 20% H₂ by volume which revealed more information about the effects of H₂ blending on a rich burn engine with 3-way catalyst. Figure 4.2.1 shows a comparison between the baseline λ-sweep and the λ-sweep with 20% H₂. There was a significant narrowing of the window of operation by 28% due to the excess NO_x produced by the engine. This is an indicator that these engine systems may need tighter control of λ in order to operate with elevated amounts of H₂ in the fuel.

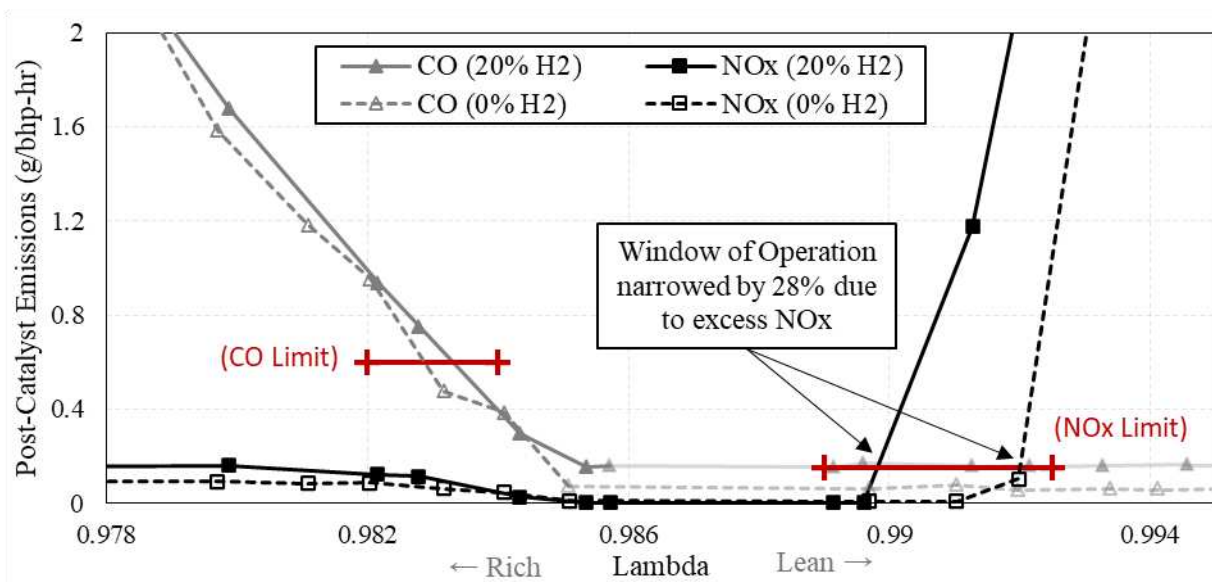


Figure 4.2.1. Post catalyst NOx and CO emissions vs. λ comparing 0% H₂ vs. 20% H₂.

An added benefit from blending H₂ into the natural gas fuel is a reduction in THCs throughout the operation window. Seen in Figure 4.2.2, THCs were reduced by at least 0.2 g/hp-hr throughout the compliance window. This is likely caused by better reaction initiation due to the increased H₂ content of the fuel, as well as an increase in NOx supplied to the catalyst providing additional oxygen to oxidize the THCs.

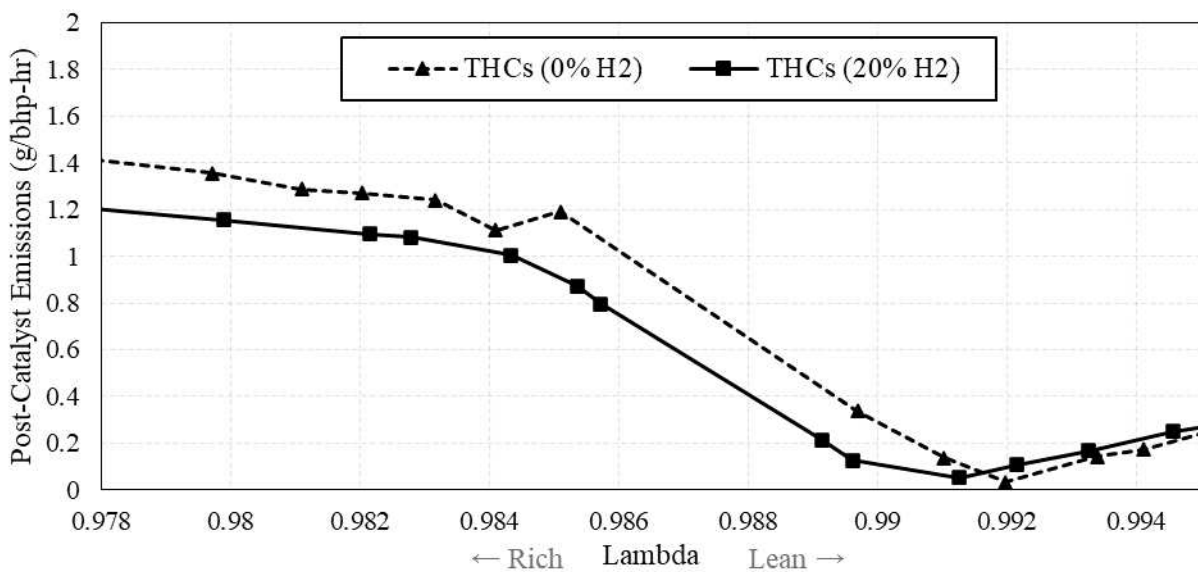


Figure 4.2.2. Post-catalyst unburned hydrocarbon (THC) emissions vs. λ , comparing fuel with and without H₂.

4.3, H₂ Concentration Transitions

While testing different concentrations of H₂ in the natural gas fuel, an observation was made during the transitions. Each time H₂ was added to the fuel stream, λ would immediately become lean and would take a minute to return to normal. The opposite would also happen when reducing the concentration of H₂ in the fuel, causing λ to run rich for a few minutes. An example of a lean transition caused by adding H₂ is shown in Figure 4.3.1, showing the change in λ as H₂ is added to the fuel.

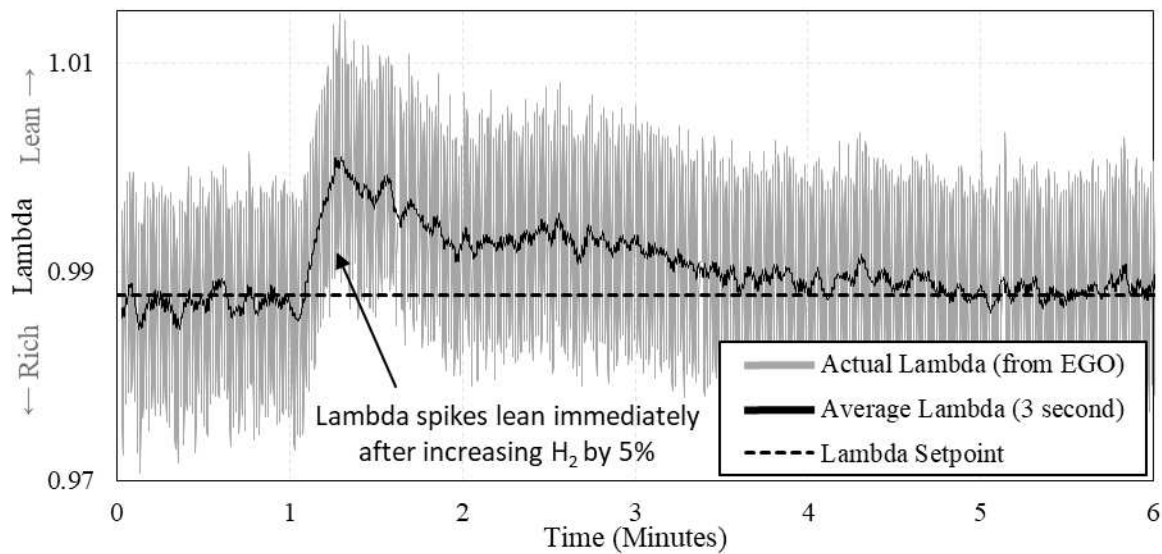


Figure 4.3.1. Example of λ vs. time after increasing H₂ from 10% to 15% by volume in the fuel.

Looking closer at this phenomena, λ transitions lean almost simultaneously as H₂ is added to the fuel, shown in Figure 4.3.2. This is happening because the stoichiometric air-fuel ratio of the fuel is changing at its chemistry changes. Changing air-fuel ratios (AFRs) and expected flow rates are shown in Table 4.3.1. Here, it can be counter intuitive to see that as H₂ is added to the fuel - the stoichiometric AFR increases, yet air flow decreases. This is because of the changing energy density of the fuel, as more H₂ is added – the fuel becomes more energy

dense by mass – requiring less fuel mass to maintain power output. The decreased demand for fuel by mass results in decreased airflow, both by mass and volumetrically.

The expected reduction in airflow is likely the cause of the lean spikes when increasing H₂ in the fuel. The moment H₂ is added to the fuel, the flow rates of air and fuel become invalid for the new fuel blend, resulting in too much air being supplied to the mixture until the engine controller can adapt.

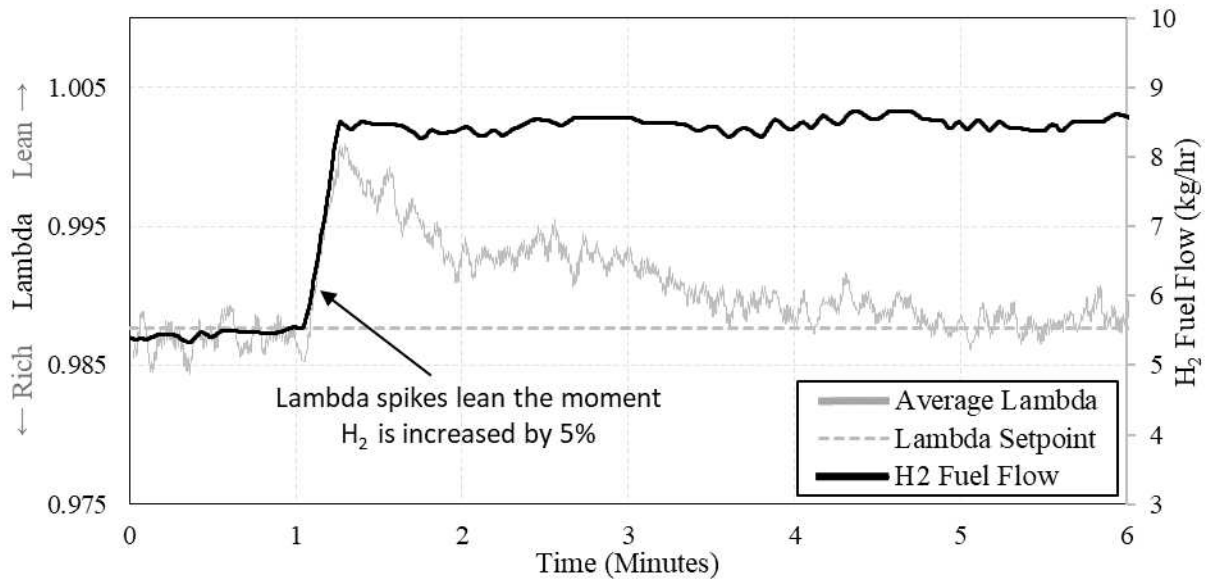


Figure 4.3.2. λ and H₂ fuel flow vs. time after increasing H₂ from 10% to 15%.

Table 4.3.1. Expected flows of methane (CH₄), H₂, and air into the engine with a load of 298kW

%H ₂ by vol.	Stoich AFR	Mass flow (kg/hr)					Volumetric flow (l/min)				
		NG (CH ₄)	H ₂	Fuel Mix	Air	Total	NG (CH ₄)	H ₂	Fuel Mix	Air	Total
0%	17.185	66.64	0	66.64	1145	1212	1693	0	1693	16115	17808
5%	17.297	65.53	0.4334	65.96	1141	1207	1665	87.61	1752	16056	17808
10%	17.419	64.34	0.8984	65.24	1137	1202	1635	181.6	1816	15993	17809
15%	17.554	63.07	1.399	64.47	1132	1196	1602	282.7	1885	15924	17809
20%	17.703	61.69	1.938	63.63	1126	1190	1567	391.8	1959	15851	17810
25%	17.869	60.2	2.522	62.72	1121	1184	1529	509.7	2039	15771	17810
30%	18.054	58.58	3.155	61.74	1115	1176	1488	637.8	2126	15685	17811

As λ would change lean or rich when increasing or decreasing H₂, there was an expected change in exhaust chemistry as well. When H₂ was removed from the fuel, λ would drift rich and a small increase in CO emissions could be observed in the post-catalyst exhaust. When H₂ was

added to the fuel, λ would stray lean, and a large spike in NOx could be observed in the post-catalyst exhaust. Large quantities of NOx were observed whenever H₂ was added to the fuel stream. An example of this is shown in Figure 4.3.3, comparing post-catalyst NOx emissions and λ vs. time.

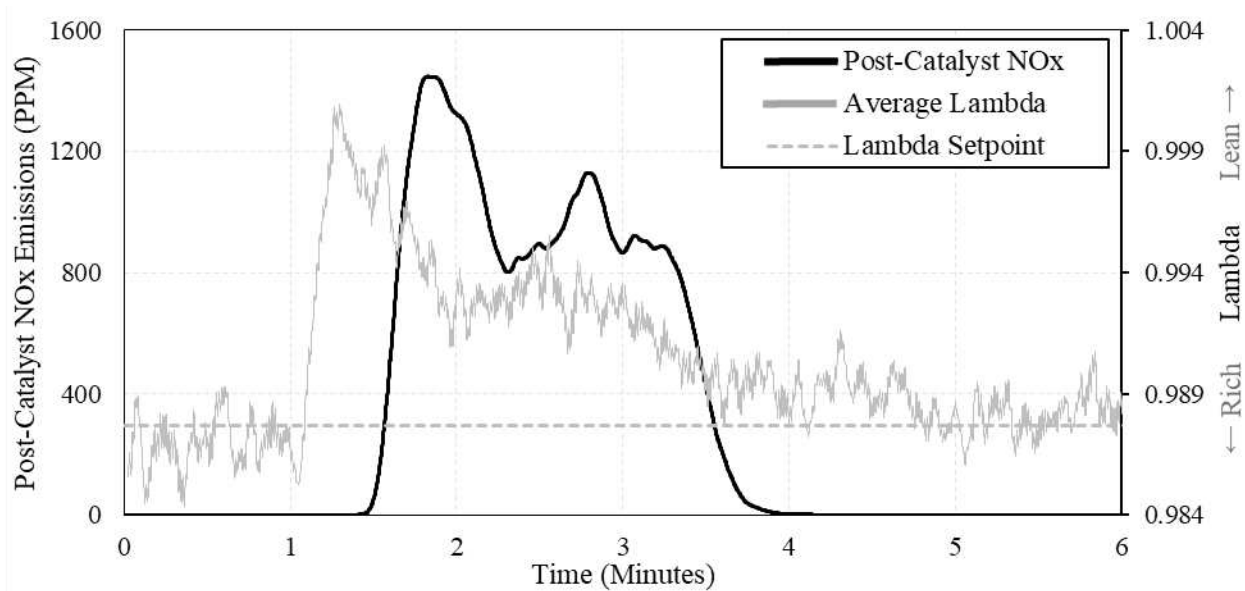


Figure 4.3.3. An example of λ and NOx emissions vs. time after H₂ increased by 5%.

It should be noted that when H₂ was removed, λ drifted rich and excess CO was emitted post-catalyst, however the quantity was typically limited. When the catalyst receives rich exhaust, it becomes less effective and allows some CO to pass by, however this transition is gradual, and CO increases proportionally to λ . The temporary rich excursions caused by removing H₂ from the fuel did not produce enough post-catalyst CO to make a significant impact or to push the engine out of compliance for a 1-hour average.

The more concerning events were the large spikes of post-catalyst NOx emissions when H₂ was added to the fuel stream. When λ strays lean, the catalyst will become saturated with oxygen, allowing NOx to pass by unaffected. This transition in the catalyst can happen quickly, and results in large post-catalyst NOx emissions. An example of the timing of these reactions is

shown in Figure 4.3.4, where we observed about a 20 second delay between λ changing lean and post-catalyst NOx emissions rising.

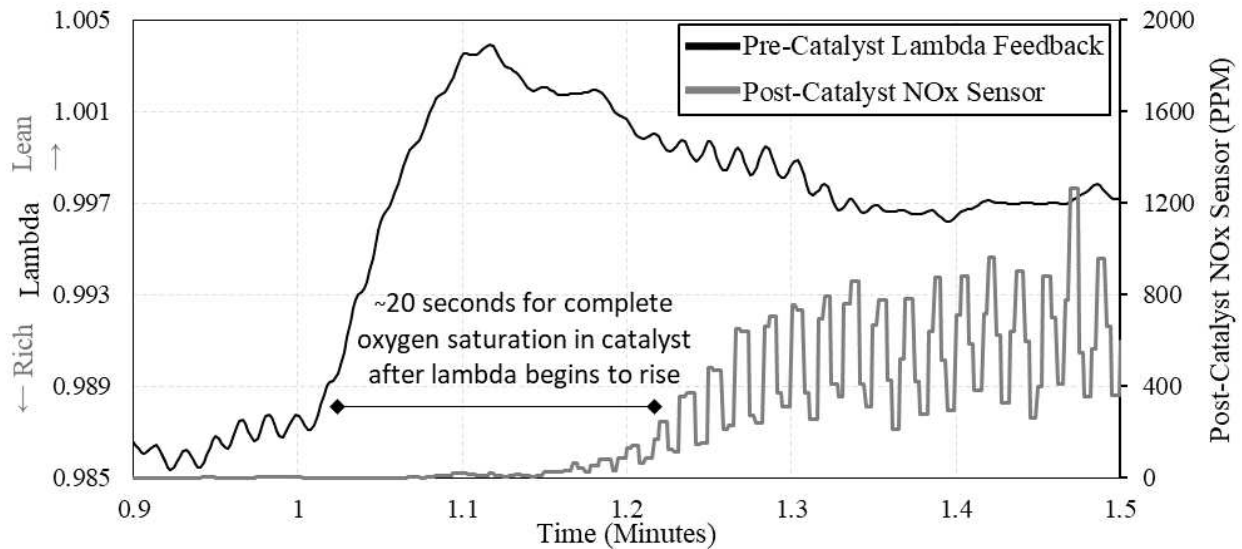


Figure 4.3.4. Comparison between when λ strays lean and the resulting increase in post-catalyst NOx emissions.

The initial observation of NOx emissions was made while conducting the initial H₂ concentration sweep. The test involved increasing H₂ by 5% increments from 0% to 30%, while allowing the engine and catalyst time to settle between data points. Each time H₂ was increased, λ would spike very lean, and a large amount of NOx was observed in the post-catalyst exhaust. At increased levels of H₂, these transitions became more dramatic, producing higher NOx emissions during each transition. A comparison between the lowest transition (0% to 5%) and the highest transition (25% to 30%) is shown in Figure 4.3.5.

The quantity of NOx produced by these events were assessed to evaluate their impact. The sum of post-catalyst NOx emissions produced from each transition event were included in 1-hour averages, assuming the engine operated normally for the remaining times. The results from these averages are shown in Figure 4.3.6 for each of the increasing 5% transitions. As can be seen, higher transitions produced more NOx than the regulation limit of 0.15 g/bhp-hr. This

could be an issue for operators required to stay under certain emissions limits if their fuel constituents change quickly.

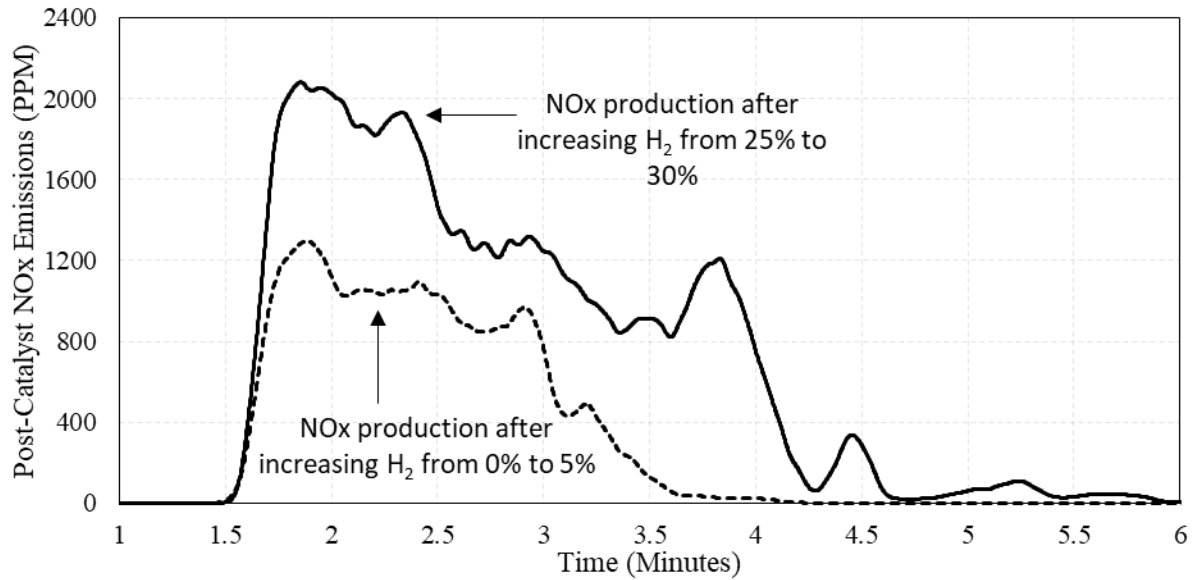


Figure 4.3.5. Comparison of NOx emissions produced from the lowest H₂ transition (0% to 5%) and the highest H₂ transition (25% to 30%).

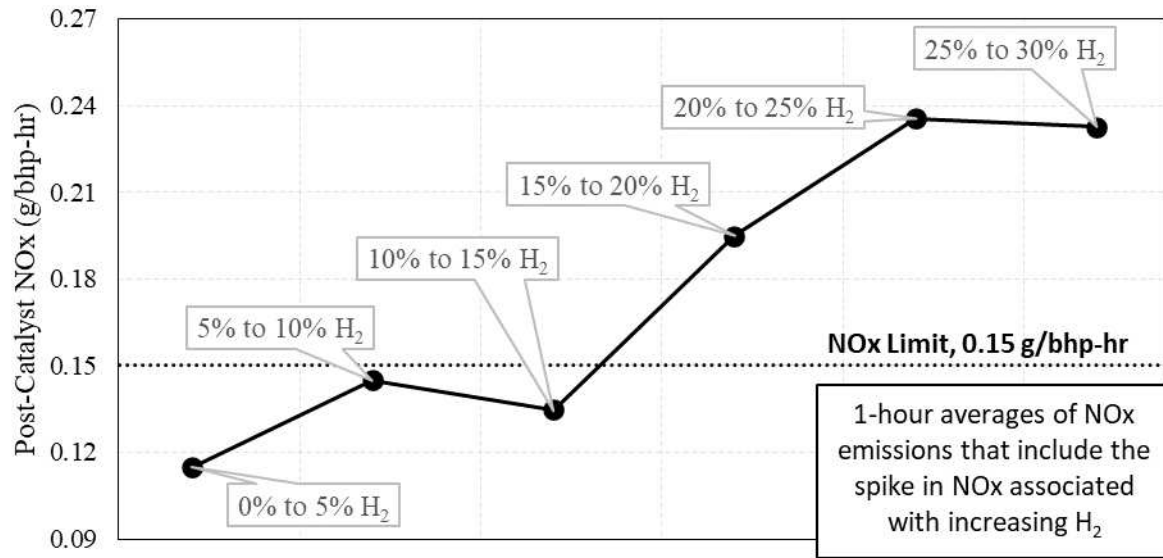


Figure 4.3.6. 1-hour NOx emission averages that include the elevated NOx production associated with increasing H₂.

The increasing impact of H₂ transitions at elevated levels can again be described by looking at the expected air-flow rates as H₂ is increased. Shown in Table 4.3.2, the magnitude of

the change in airflow increases as H₂ increases, resulting in more dramatic lean excursions each time H₂ increases.

Table 4.3.2. *Expected flow rates of air for increased H₂ in the NG fuel.*

%H ₂ by vol.	Stoich AFR	Air (kg/hr)	Δ Air	Air (l/min)	Δ Air
0%	17.185	1145		16115	
5%	17.297	1141	-4	16056	-59
10%	17.419	1137	-4	15993	-63
15%	17.554	1132	-5	15924	-69
20%	17.703	1126	-6	15851	-73
25%	17.869	1121	-5	15771	-80
30%	18.054	1115	-6	15685	-86

4.4, LECM Response Time (PID)

Further investigation into the engine’s response to transitioning H₂ led directly to the engine’s controls. The quantity of post-catalyst NO_x produced directly correlated with how long it took for the engine to return λ to normal. By that line of thinking, the more quickly the engine can return to normal, the less NO_x will be produced by changing the fuel constituents.

The CG137-8 engine-set was originally installed at CSU in 2018 and was later retrofit with a Woodward Large Engine Control Module (LECM) with Real Time Combustion Detonation Control (RTCDC). Along with the new LECM, the engine was also fit with a new Woodward electronic fuel regulator (EFR) and F-series throttle. This engine control scheme gave the LECM full fuel authority with control of fuel flow, fuel/air mixture flow, and spark timing.

Control software was written for this system using Woodward MotoHawk in 2021 when the engine was upgraded with the new LECM [12]. In this software, feedback loops were written to control the engine speed and engine λ . Two control loops were set up as proportional-integral-derivative controllers (PID), one loop was written to control the engine’s speed (RPM), and the second was written to maintain the engine’s λ . A flowchart for a typical PID control loop is shown in Figure 4.4.1. When the engine changes load or speed, the RPM control loop adjusts the

flow of fuel and the air-fuel mixture using the electronic fuel valve and the throttle to meet the new demand and hold speed stable. At the same time, the λ control loop assesses EGO sensor feedback to evaluate λ and adjusts the fuel flow using the electronic fuel valve to meet the desired λ setpoint. If these two control loops responded at the same speed they would constantly interfere with each other. To address this conflict, the speed control loop was originally tuned to respond twice as quickly as the λ control loop [12], because engine operation takes priority.

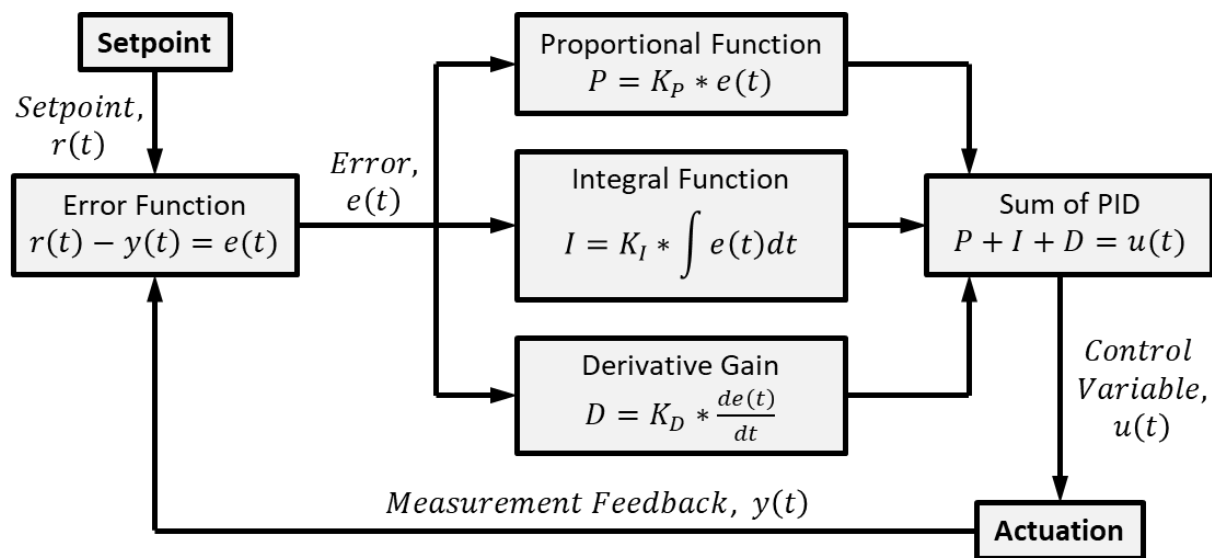


Figure 4.4.1. Flowchart showing a typical PID feedback loop.

These PID control loops came into focus in the current project when investigating engine response to changing fuel constituents. When H_2 was added to the fuel, the engine’s speed would drop by less than 10 RPMs and returned to normal within 10 seconds, indicating the RPM control loop was doing its job as intended. An example showing the change in engine speed after a 5% addition of H_2 is shown in Figure 4.4.2. The λ control loop was thought to have room for improvement, as it would take minutes for the engine to adapt to the new fuel blend and for λ to return to the setpoint.

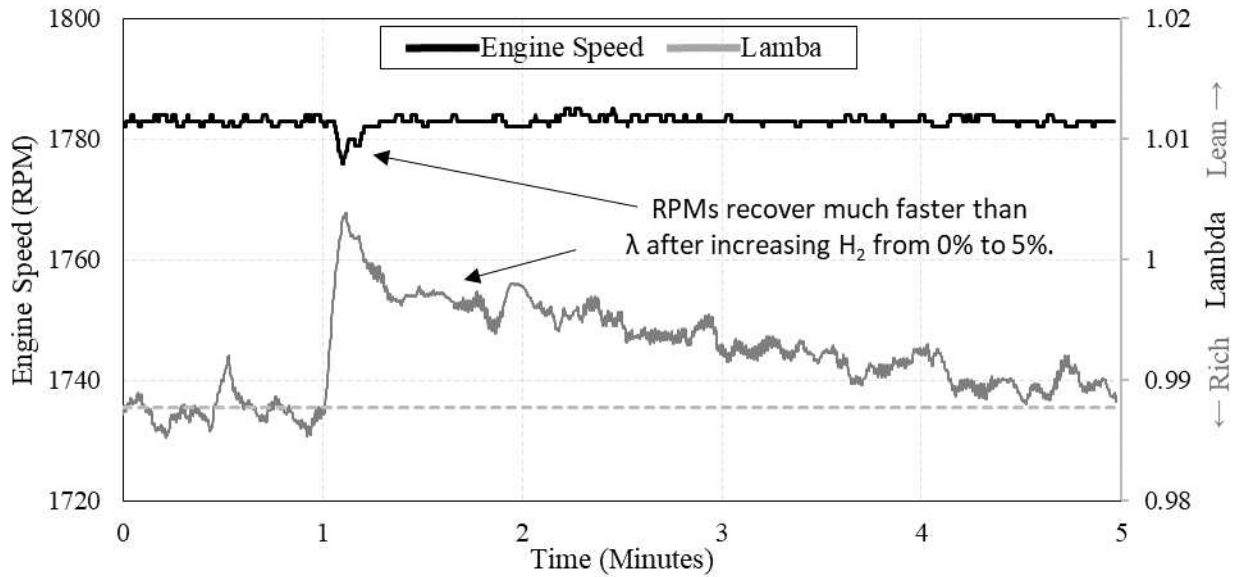


Figure 4.4.2. Comparison between engine speed and λ after an increase in H_2 in the fuel supply.

We can see the response of the two PID loops when looking at the behavior of the electronic fuel valve during an increasing H_2 transition. Shown in Figure 4.4.3, immediately after H_2 is added – the fuel valve opens quickly to maintain engine speed. Then, the fuel valve continues to open more gradually to return λ to the setpoint.

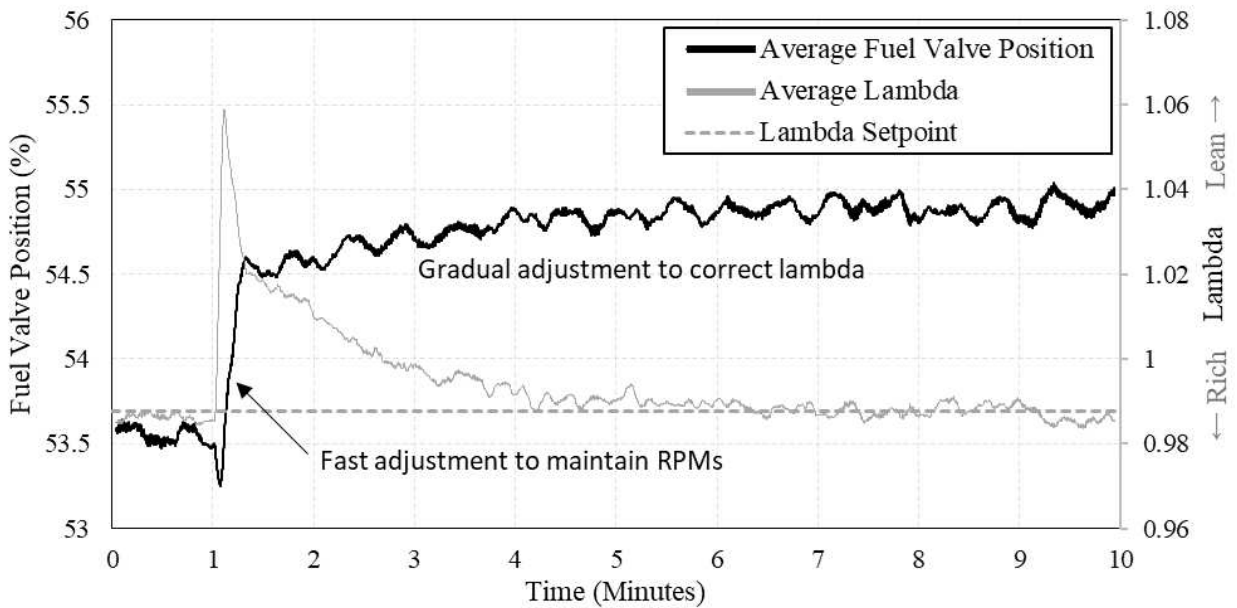


Figure 4.4.3. Electronic fuel valve demand and λ during an increasing H_2 transition.

Changing the PID values of the λ feedback loop changed the response times of the engine when H_2 was added to the fuel stream. An example comparison between two different λ responses is shown in Figure 4.4.4. The only difference between the two tests shown in Figure 4.4.4 is a different P-value setting in the λ PID feedback loop. The different λ responses shown in Figure 4.4.4 produce significantly different amounts of post-catalyst NO_x . Figure 4.4.5 shows the different NO_x emissions from the same two tests.

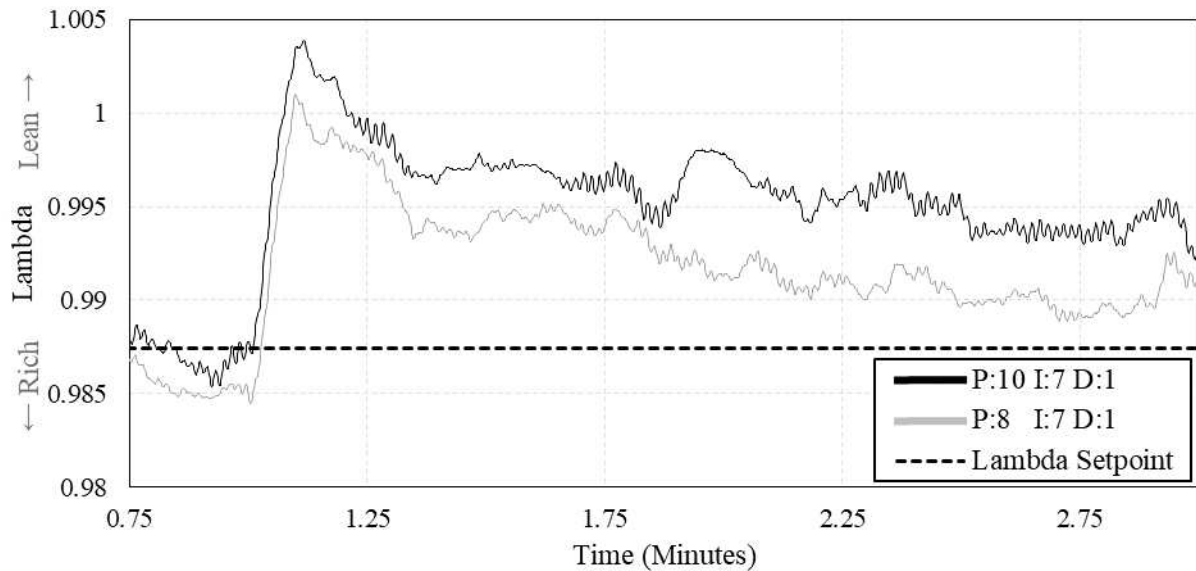


Figure 4.4.4. Comparison between two different λ responses when H_2 was increased from 0% to 5%. The only change between these tests is a different P-value setting in the λ PID control loop.

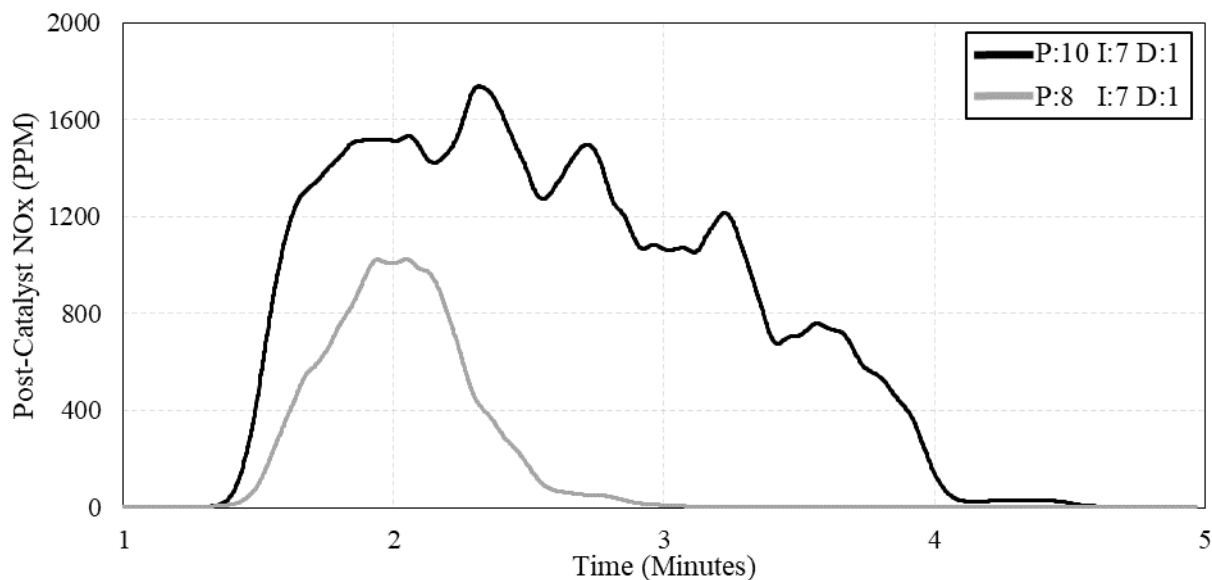


Figure 4.4.5. Comparison between NOx emissions from the transitions shown in Figure 4.4.4.

Recognizing that the engine controller may require tuning, an improvised test plan was created to vary the PID values to examine different λ responses. First, the proportional values were varied while holding the integral and derivative values constant. For each P-value, the engine was subjected to an increase in H₂ from 0% to 5%, and post-catalyst NOx emissions were recorded to evaluate the different responses. Results from the initial P-sweep are shown below in Figure 4.4.6.

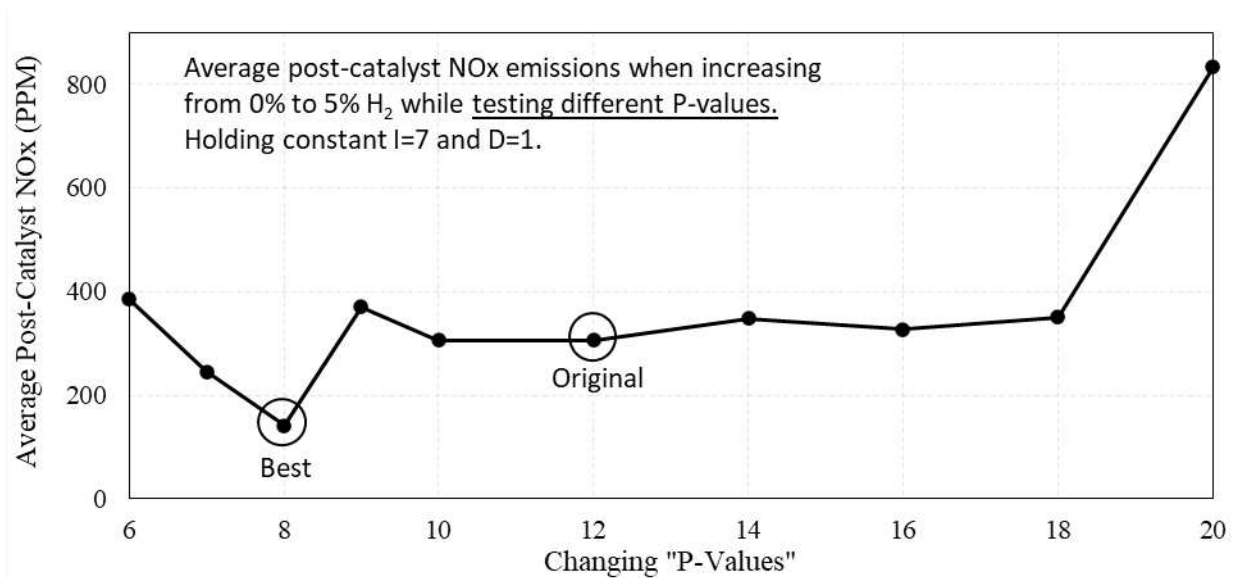


Figure 4.4.6. Estimated averages of post-catalyst NOx emissions during 0% to 5% H₂ transitions while operating with different P-value settings in the λ PID control loop.

Next, the integral value was varied while holding the proportional and derivative terms constant, using the optimal value for proportional from the initial sweep of P=8. Results from the I-sweep are shown in Figure 4.4.7.

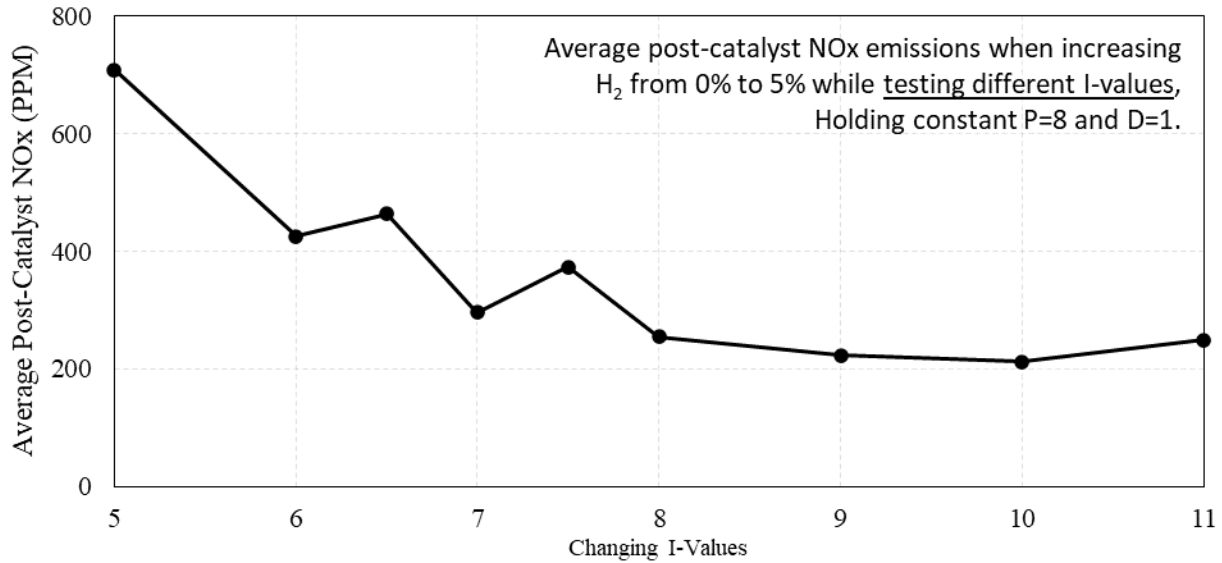


Figure 4.4.7. Estimated averages of post-catalyst NOx emissions during a 0% to 5% H₂ transition while operating with different I-value settings in the λ PID control loop.

Some of the transitions from the proportional and integral sweeps were evaluated to see if these transitions were violating regulation limits for a 1-hour average. Average post-catalyst NOx emissions were weighted for their collection time and added to the average NOx emissions from stable operation with 5% H₂ from previous tests. Results from this evaluation are shown in Figure 4.4.8. Here, it can be seen that some engine controllers can exceed one-hour average emissions limits with as little as a 5% increase in H₂ if the transition is sudden. Some engine controllers may need to be tuned or upgraded in order to tolerate elevated levels of H₂.

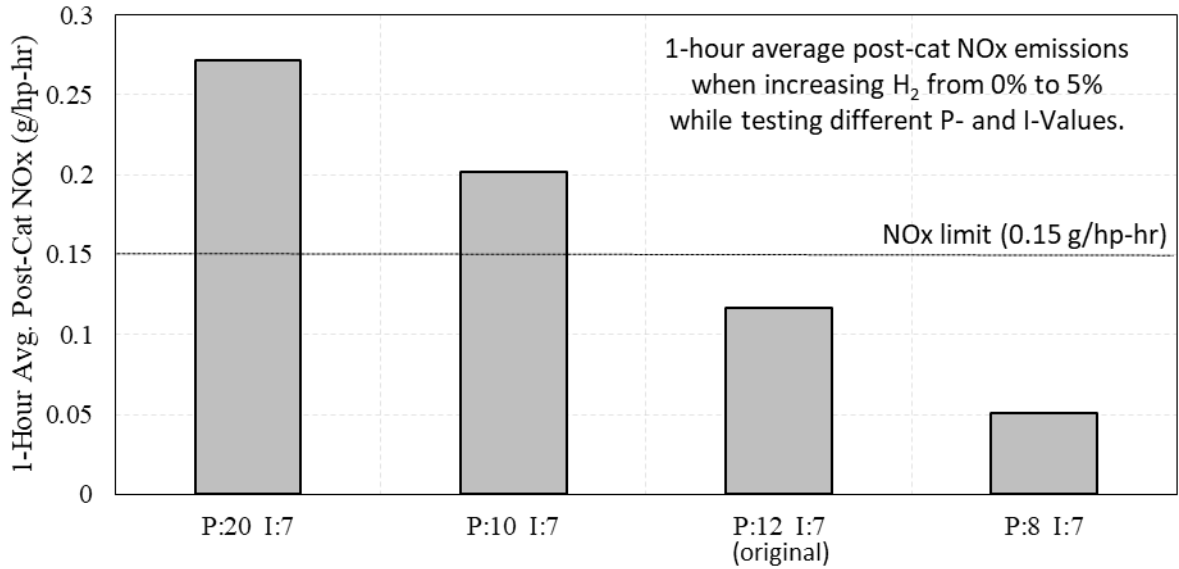


Figure 4.4.8. 1-hour average post-catalyst NOx emissions when increasing H₂ from 0% to 5% while testing different proportional and integral settings.

Next, the optimal proportional and integral values were applied during larger transitions of H₂ from 0% to 20%, to see if it was possible to keep emissions under regulation limits for such a large transition. The original values from previous testing (P=12, I=7) were evaluated also as a comparison. Results from this evaluation are shown in Figure 4.4.9. Here, it was not possible for the engine to tolerate a 20% increase in H₂ without violating regulation NOx limits for a 1-hour average, no matter the PID settings.

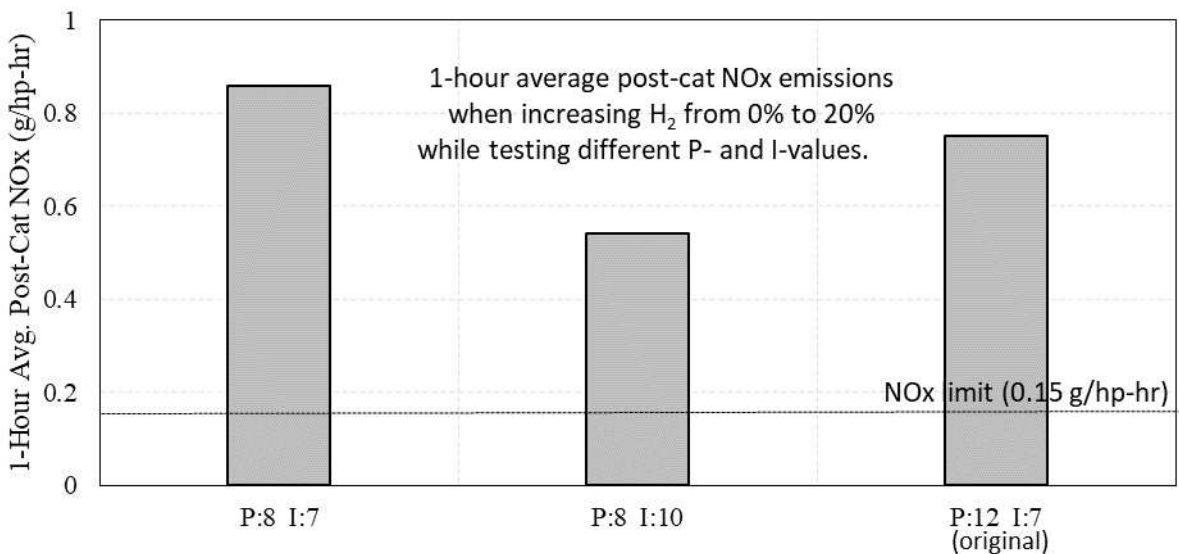


Figure 4.4.9. 1-hour average post-cat NOx emissions when increasing H₂ from 0% to 20% while testing different proportional and integral settings.

The fastest recovery from a 0% to 20% increase in H₂ is shown in Figure 4.4.10. Peak NOx and peak λ are both significantly higher than any previous testing involving a 5% H₂ transition. The time it takes for the engine to recover λ is dictated by the response of the engine controller, however, the initial change in λ and the peak value of λ are caused by the size of the transition in H₂. Because the fuel transition is so large and so sudden, it is likely not possible for the engine system to tolerate a sudden increase in H₂ by 20% without violating regulation limits for a 1-hour average, even with the best possible PID tuning.

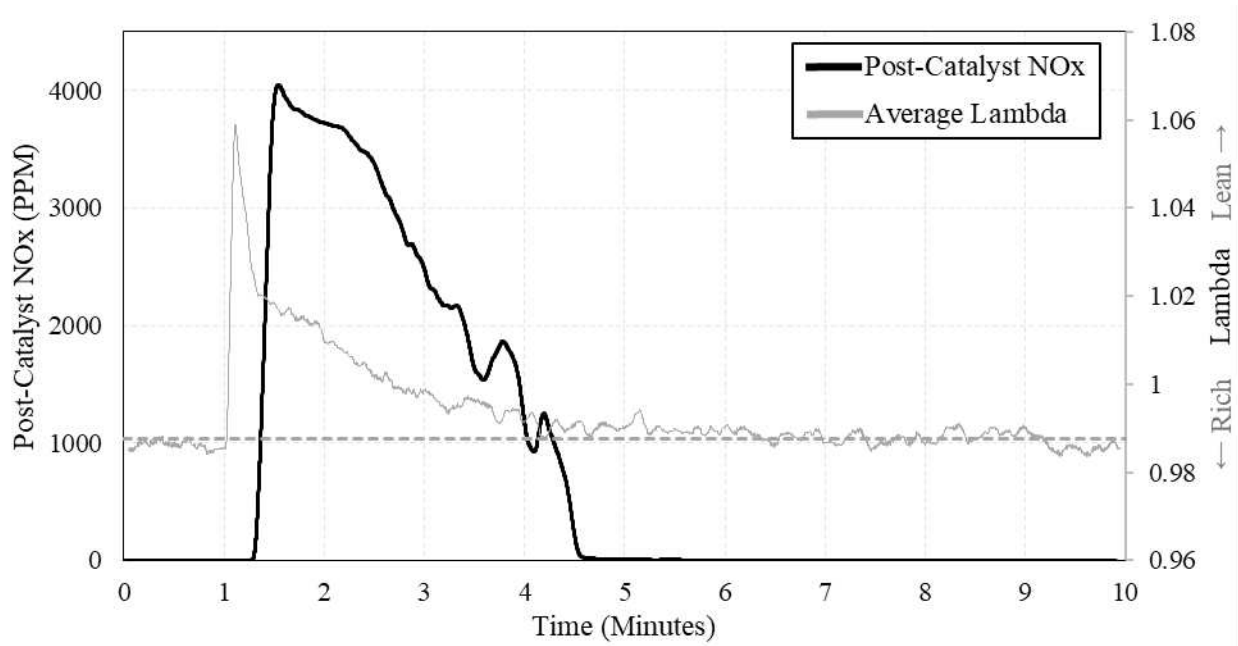


Figure 4.4.10. Post-catalyst NOx and λ vs. time during a 0% to 20% increase in H₂.

Finally, all the tests involving a 20% transition of H₂ were evaluated on a 3-hour average, assuming the engine experienced a 20% sudden transition and operated normally for the remaining time. The results of this evaluation are shown in Figure 4.4.11. While some came close, none of the tests stayed under the regulation limit for even a 3-hour sample time.

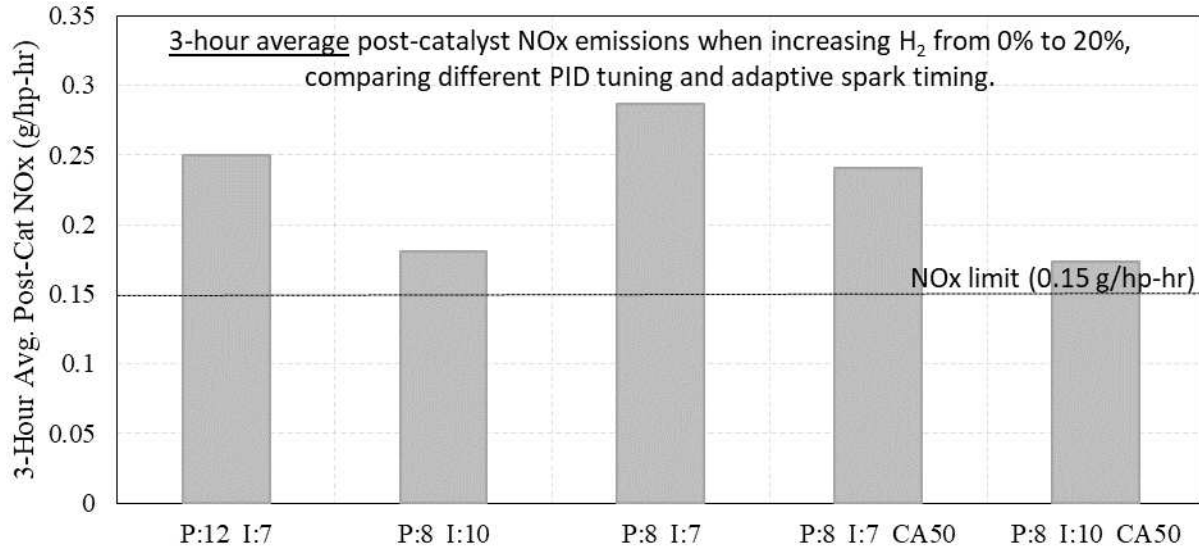


Figure 4.4.11. 3-hour average post-catalyst NOx emissions when increasing H₂ from 0% to 20% while testing different proportional and integral settings.

The intended takeaway from this chapter is that the engine controller dictates how quickly the engine adjusts to changing fuel blends, and that many engine controllers may need to be upgraded or tuned for faster λ response. The PID values shown in this chapter were only valid for the engine setup used in testing and may vary from system to system.

CONCLUSION

The main objective of this project was to blend gaseous H₂ with the natural gas fuel supply going to a “rich burn” engine with a 3-way catalyst, and to observe the changes in exhaust chemistry for various concentrations of H₂. Exploration into improving air-fuel controls was an objective as well, with the intention of improving engine emissions.

A natural gas Caterpillar CG137-8 industrial “rich burn” engine with a 3-way catalyst was used for testing H₂-NG fuel blending. While operating the engine, H₂ was added to the NG fuel up to 30% by volume. Then, a λ -sweep was conducted while running with a 20% blend of H₂, to define the new limits of the window of operation. Finally, LECM response was assessed while abruptly changing fuel blends, which lead to exploration into PID tuning of the engine.

Results from the H₂ concentration sweep indicate that the engine setup used for testing can tolerate up to 30% H₂ by volume in the NG fuel stream without exceeding emissions limits during steady operation.

- Previous research projects at CSU have observed that some engines with narrow band λ sensors can fail due to high NO_x emissions with as little as 5% H₂.
- Combustion behavior changed, with ignition delay shortening and peak pressure increasing as H₂ was added.
- There was a significant reduction in GHG emissions, with NG flow reduced by 7.3% and GHG emissions reduced by 8.1% with a 20% blend of H₂ by volume.
- With increasing H₂, engine-out NO_x increased, and engine-out CO decreased.
- With increasing H₂, changes in post-catalyst NO_x and CO were insignificant.

Carrying out a λ sweep while operating with a 20% blend of H₂ revealed that the window of operation narrowed by ~28% due to excess NO_x production. This is an indication that similar engine systems may need to operate with tighter control of λ in order to operate with elevated amounts of H₂ in the fuel.

While testing increasing blends of H₂, large emissions of NO_x were observed whenever H₂ was abruptly increased because the transition would cause the engine to run lean for a short time. This led to investigation into sharp changes in H₂ concentrations. As the fuel constituents change, the rate of airflow must also change to meet the required AFR for the new fuel blend. Whenever the H₂ fuel concentration changed, it took some time for the engine controller to adapt and adjust the airflow.

- Increasing H₂ in the fuel stream required less airflow to the engine. Whenever H₂ was abruptly increased, λ would temporarily stay lean until the engine controller could adapt.
- The further λ strayed from the setpoint and the longer it took for the engine controller to return it to normal - the more post-catalyst emissions were observed.
- The temporary lean excursions due to increasing H₂ in the fuel caused a corresponding increase in post-catalyst NO_x. The temporary spikes in NO_x could exceed 1-hour average emissions limits with as little as a 5% increase in H₂.
- Similar behavior was observed when reducing H₂, causing temporary rich operation, and a small increase in post-catalyst CO. However, the increase in CO was insignificant and did not cause the engine to violate our CO emission limit.

Further investigation into the engine's response to transitioning H₂ led directly to the engine's controls. The performance of the engine controller dictated how long it took for λ to return to normal and the quantity of post-catalyst NO_x produced from changing H₂ blends.

- The engine controller was previously set up to use PID feedback control loops for the engine speed and λ . Tuning the PID parameters affected how quickly the engine adapted to changing fuel blends.
- Post-catalyst NO_x production associated with a 5% increase in H₂ was reduced by over 50% after simply tuning the λ PID control loop. This shows that engine controller feedback loops may need to be improved for some engines that will operate with H₂.
- Engine operators should be aware that poor PID tuning can result in post-catalyst NO_x emissions that will violate limits with as little as 5% H₂ added to the fuel.
- The engine could not tolerate a sharp increase in H₂ by 20% without violating even the 3-hour average NO_x limit, regardless of PID tuning. While adding 20% H₂ as a step-change is unusual, this could be an issue for engine operators located near H₂ injection points on the NG pipeline network or for operators planning to blend H₂ on their own.

Overall, blending H₂ with NG on our “rich burn” engine was a success. During steady operation, GHG emissions were significantly reduced while post-catalyst NO_x and CO were relatively unchanged. Controlling λ may be an issue for some operators, but this engine setup with an advanced λ control system tolerated H₂ well. Some unique scenarios involving sharp increases in H₂ may be of concern to some operators, however most operators will not be worried about abrupt increases in H₂.

REFERENCES

First appearing in motivation:

- [1] “DOE Establishes Bipartisan Infrastructure Law's \$9.5 Billion Clean Hydrogen Initiatives”, *energy.gov*, February 15, 2022, <https://www.energy.gov/articles/doe-establishes-bipartisan-infrastructure-laws-95-billion-clean-hydrogen-initiatives>
- [2] “HyBlend: Opportunities for Hydrogen Blending in Natural Gas Pipelines”, *energy.gov*, Office of Energy Efficiency & Renewable Energy, accessed January 2023, <https://www.energy.gov/sites/default/files/2021-08/hyblend-tech-summary.pdf>
- [3] "Climate Commitment to Net Zero 2045", *Southern California Gas Company*, a subsidiary of Sempra, released March 23, 2021, accessed January 2023, https://www.socalgas.com/sites/default/files/2021-03/SoCalGas_Climate_Commitment.pdf
- [4] H. Petrizzo, "Joint Utility Preliminary Hydrogen Injection Standard Application, Chapter 3, Hydrogen Blending Demonstration Program" *Southern California Gas Company*, a subsidiary of Sempra, application submitted November 20, 2020, https://www.socalgas.com/sites/default/files/2020-11/H2_Application-Chapter_3_H2_Demonstration_Program.pdf

First appearing in engine/catalyst literature review:

- [5] Turns, S., “An Introduction to Combustion Concepts and Applications, 3rd Ed.”, *McGraw-Hill Education*, 2011, ISBN 978-1-25-902594-5
- [6] “Ground-level Ozone Basics” *epa.gov*, last updated June 2022, <https://www.epa.gov/ground-level-ozone-pollution/ground-level-ozone-basics#formation>

- [7] Lott, P., Deutschmann, O., “Lean-Burn Natural Gas Engines: Challenges and Concepts for an efficient Exhaust Gas Aftertreatment System”, *Emission Control Science and Technology*, 2021, <https://doi.org/10.1007/s40825-020-00176-w>
- [8] Einewall, P., Tunestal, P., Johansson B., “Lean Burn Natural Gas Operation vs. Stoichiometric Operation with EGR and a Three Way Catalyst” *Lund University*, published in SAE Special Publications, 2005, DOI: 10.4271/2005-01-0250
- [9] Kirkpatrick, A.T., “Internal Combustion Engines – Applied Thermosciences, 4th Edition”, *Wiley*, 2021, ISBN 9781119454557
- [10] Heywood, J.B., “Internal Combustion Engine Fundamentals, 2nd Edition”, *McGraw-Hill Education*, 2018, ISBN 978-1-260-11610-6
- [11] Defoort, M., Olsen, D., Willson, B., “The effect on air-fuel ratio control strategies on nitrogen compound formation in three-way catalysts” *International Journal of Engine Research*, Volume 5, Number 1, 2004, <https://doi-org.ezproxy2.library.colostate.edu/10.1243/146808704772914291>
- [12] Jones, A.L., Olsen, D.B., “Evaluation of Advanced Air-Fuel Ratio Control Strategies and their Effects on Three-Way Catalysts in a Stoichiometric, Spark Ignited, Natural Gas Engine”, *Colorado State University*, MS Thesis, May 2021

First appearing in H₂ blending literature review:

- [13] Gersen, S., Anikin, N.B., Mokhov, A.V., Levinsky, H.B., "Ignition Properties of Methane/Hydrogen Mixtures in a Rapid Compression Machine", *International Journal of Hydrogen Energy*, Volume 33, Issue 7, April 2008, <https://doi.org/10.1016/j.ijhydene.2008.01.017>

- [14] Brower, M., Peterson, E.L., Metcalfe, W., Curran, H.J., Furl, M., Bourque, G., Aluri, N., Guthe, F., "Ignition Delay Time and Laminar Flame Speed Calculations for Natural Gas/Hydrogen Blends at Elevated Pressures", *The Journal of Engineering for Gas Turbines and Power*, January 2013, [https://doi-org.ezproxy2.library.colostate.edu/10.1115/1.4007763](https://doi.org.ezproxy2.library.colostate.edu/10.1115/1.4007763)
- [15] Xudong, Z., Xiaoyan, L., Wang, Y., Daming, L., Tian, Z., "Comparative Study on Combustion and Emission Characteristics of Methanol/Hydrogen, Ethanol/Hydrogen and Methane/Hydrogen Blends in High Compression Ratio SI Engine", *Fuel*, Volume 267, May 2020, <https://doi.org/10.1016/j.fuel.2020.117193>
- [16] Akansu, S.O., Kahraman, N., Ceper, B., "Experimental Study on a Spark Ignition Engine Fuelled by Methane-Hydrogen Mixtures", *International Journal of Hydrogen Energy*, Volume 32, Issue 17, December 2007, <https://doi.org/10.1016/j.ijhydene.2007.05.034>
- [17] Ghotge, P., Olsen, D.B., "Impact of H₂-NG Blending on Lambda Sensor NSCR Control and Lean Burn Emissions", *Colorado State University*, MS Thesis, November 2015

First appearing in body:

- [18] "Understanding SCAQMD Air Quality Rules for Engines" *Southern California Gas Company*, a subsidiary of Sempra, accessed January 2023, https://www.socalgas.com/documents/business/aq_rules_engines.pdf
- [19] Karim, G.A., Wierzba, I., Al-Alousi, Y., "Methane-Hydrogen Mixtures as Fuels", *International Journal of Hydrogen Energy*, Volume 21, Issue 7, July 1996, [https://doi.org/10.1016/0360-3199\(95\)00134-4](https://doi.org/10.1016/0360-3199(95)00134-4)
- [20] Xudong, Z., Xiaoyan, L., Wang, Y., Daming, L., Tian, Z., "Comparative Study on Combustion and Emission Characteristics of Methanol/Hydrogen, Ethanol/Hydrogen and

Methane/Hydrogen Blends in High Compression Ratio SI Engine", *Fuel*, Volume 267,
May 2020, <https://doi.org/10.1016/j.fuel.2020.117193>

[21] "Importance of Methane", *US Environmental Protection Agency*, accessed January 2023
<https://www.epa.gov/gmi/importance-methane>

APPENDICES

APPENDIX A, EXAMPLES FROM DATA COLLECTION

Engine RPM	Power [kW]	Torque [N-m]	THC [ppm]	NOx [ppm]	O2 [%]	CO2 [%]	CO [ppm]	Jacket Water In [C]	Jacket Water Out [C]	Dyno In [C]	Dyno Out [C]
1782	295	1580	-9.2	3.85	-0.31	10.57	288	59.77456284	87.2592392	13.42305279	33.65399551
1782	295	1580	-9.2	3.87	-0.31	10.57	287	59.77456284	87.2592392	13.42305279	33.65399551
1782	295	1580	-9.2	3.87	-0.31	10.57	287	59.77456284	87.2592392	13.42305279	33.65399551
1782	295	1581	-9.2	3.87	-0.31	10.57	287	59.77456284	87.2592392	13.42305279	33.65399551
1782	295	1581	-9.2	3.87	-0.31	10.57	287	59.77456284	87.2592392	13.42305279	33.65399551
1782	295	1583	-9.2	3.87	-0.31	10.57	287	59.77456284	87.2592392	13.42305279	33.65399551
1782	295	1583	-9.2	3.87	-0.31	10.57	287	59.77456284	87.2592392	13.42305279	33.65399551
1782	295	1583	-9.2	3.9	-0.31	10.57	287	59.98873138	87.28665161	13.3814373	33.62504578
1782	295	1583	-9.2	3.92	-0.31	10.57	283	59.98873138	87.28665161	13.3814373	33.62504578
1782	295	1583	-9.2	3.92	-0.31	10.57	283	59.98873138	87.28665161	13.3814373	33.62504578
1782	295	1584	-9.2	3.92	-0.31	10.57	283	59.98873138	87.28665161	13.3814373	33.62504578
1782	295	1584	-9.2	3.91	-0.31	10.57	282	59.98873138	87.28665161	13.3814373	33.62504578
1782	295	1584	-9.2	3.91	-0.31	10.57	282	59.98873138	87.28665161	13.3814373	33.62504578
1783	296	1583	-9.2	3.91	-0.31	10.57	282	59.98873138	87.28665161	13.3814373	33.62504578
1783	296	1583	-9.2	3.91	-0.31	10.57	282	59.98873138	87.28665161	13.3814373	33.62504578
1783	296	1583	-9.2	3.91	-0.31	10.57	282	59.98873138	87.28665161	13.3814373	33.62504578
1783	296	1583	-9.2	3.92	-0.31	10.57	277	59.98873138	87.28665161	13.3814373	33.62504578
1783	296	1583	-9.2	3.94	-0.31	10.57	277	59.98873138	87.28665161	13.3814373	33.62504578

ECM_NOx	ManifoldAirPress_kPa	MassAirFlow_kg/hr	ThrottlePosition	H2 Flow [kg/hr]	Combined Fuel Flow [kg/hr]	Time[sec]	Time
0.493537694	179.0679932	1293.890015	53.30331421	0.050149466	51.05451683	3757511527	01/25/2023 10:12:07.229 AM
0.493537694	179.0679932	1293.890015	53.30331421	0.050114928	51.05448229	3757511527	01/25/2023 10:12:07.295 AM
0.493537694	179.0679932	1293.890015	53.30331421	0.050114928	51.05448229	3757511527	01/25/2023 10:12:07.361 AM
0.552285492	179.1818237	1294.759521	52.91563416	0.05008039	51.05444775	3757511527	01/25/2023 10:12:07.427 AM
0.552285492	179.1818237	1294.759521	52.91563416	0.050045851	51.05441321	3757511527	01/25/2023 10:12:07.494 AM
0.552285492	179.1818237	1294.759521	52.91563416	0.050045851	51.05441321	3757511528	01/25/2023 10:12:07.559 AM
0.552285492	179.1818237	1294.759521	52.91563416	0.050011313	51.05437867	3757511528	01/25/2023 10:12:07.625 AM
0.552285492	179.1818237	1294.759521	52.91563416	0.050011313	51.05437867	3757511528	01/25/2023 10:12:07.691 AM
0.915296018	179.2136536	1296.349121	52.9310379	0.049994044	51.0543614	3757511528	01/25/2023 10:12:07.757 AM
0.915296018	179.2136536	1296.349121	52.9310379	0.049976775	51.02049256	3757511528	01/25/2023 10:12:07.823 AM
0.915296018	179.2136536	1296.349121	52.9310379	0.049976775	51.02049256	3757511528	01/25/2023 10:12:07.890 AM
0.548479021	179.0353394	1293.359131	53.00836182	0.049959506	51.02047529	3757511528	01/25/2023 10:12:07.956 AM
0.548479021	179.0353394	1293.359131	53.00836182	0.049959506	51.02047529	3757511528	01/25/2023 10:12:08.021 AM
0.548479021	179.0353394	1293.359131	53.00836182	0.049959506	51.02047529	3757511528	01/25/2023 10:12:08.089 AM
0.548479021	179.0353394	1293.359131	53.00836182	0.049959506	51.02047529	3757511528	01/25/2023 10:12:08.154 AM
0.552571952	179.1268158	1294.84021	53.04656219	0.049942237	51.02045802	3757511528	01/25/2023 10:12:08.220 AM
0.552571952	179.1268158	1294.84021	53.04656219	0.049942237	51.02045802	3757511528	01/25/2023 10:12:08.286 AM
0.552571952	179.1268158	1294.84021	53.04656219	0.049924968	51.02044075	3757511528	01/25/2023 10:12:08.352 AM
0.588577867	178.9126282	1294.963257	52.81549835	0.049907699	51.02042348	3757511528	01/25/2023 10:12:08.418 AM

Figures A-1 and A-2. Example data collected from the LabVIEW control program that monitors sensors on the engine and controls facility operations.

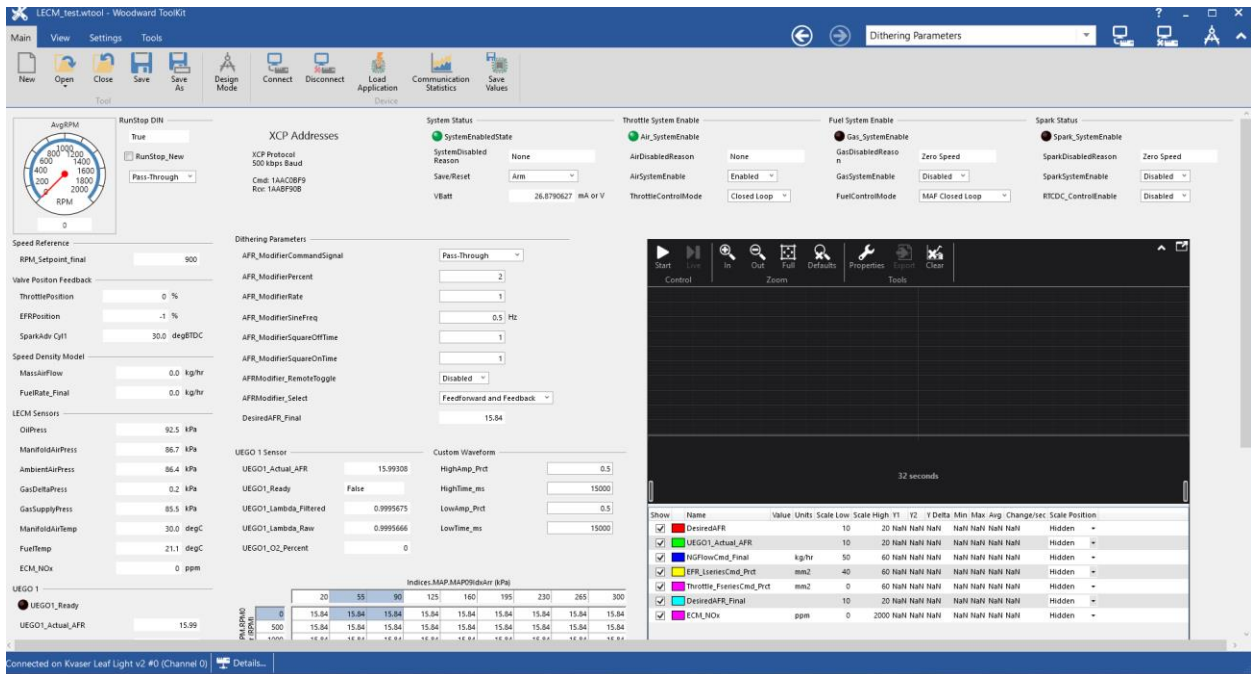


Figure A-5. Screenshot of the user interface for the Woodward Motohawk Toolkit interacting with the Large Engine Control Module. This interface allowed us to change operating parameters while running the engine and to collect data from the LECM.

APPENDIX B, HYDROGEN DISTRIBUTION SYSTEM DESIGN AND FABRICATION

APPENDIX B.1 SYSTEM DESCRIPTION

The H₂ distribution system delivers H₂ fuel to the CG137-8 engine, and in the future will be upgraded to service other engines within the Powerhouse Engine Laboratory. Hydrogen is supplied by storage trailers outside of the building, and stainless-steel tubing is used to pipe the gas into the lab space. Inside the lab space, the high pressure H₂ gas is regulated down to low pressure and supplied to the engine fuel for blending with natural gas.

APPENDIX B.2 SPECIFICATIONS

- H₂ supplied by storage trailer can range up to 3600psi
- H₂ to be blended with natural gas fuel at 15 psi
- Maximum H₂ flow rate for CG137-8 is 22.5 standard cubic feet per minute (scfm)
- H₂ flow rate must be accurately measured and steadily controlled
- H₂ storage trailer must be 20' from building openings
- H₂ storage trailer must be protected by fencing
- No other fuel storage can be within 16' of H₂ storage trailer
- H₂ delivery system tubing should allow flow rates as high as 100 scfm

APPENDIX B.3 SCHEMATICS AND PICTURE

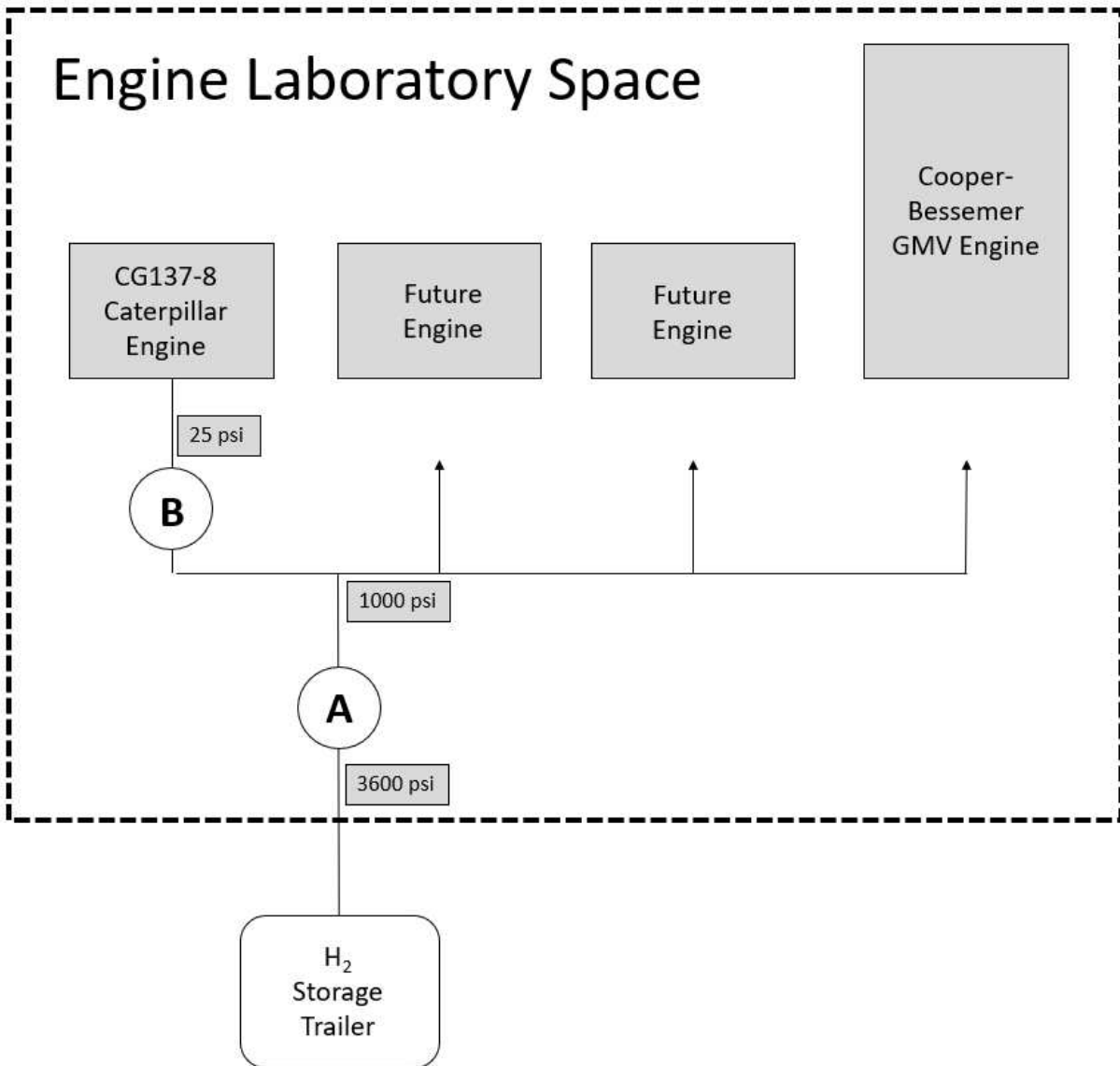


Figure B-1. Overview Schematic, showing the layout of the hydrogen distribution system in the lab space. The system is operational to supply H₂ fuel to the CG137-8 engine and will be upgraded to supply fuel to the GMV engine and two more engines in the future. Special callouts for assemblies at locations A and B.

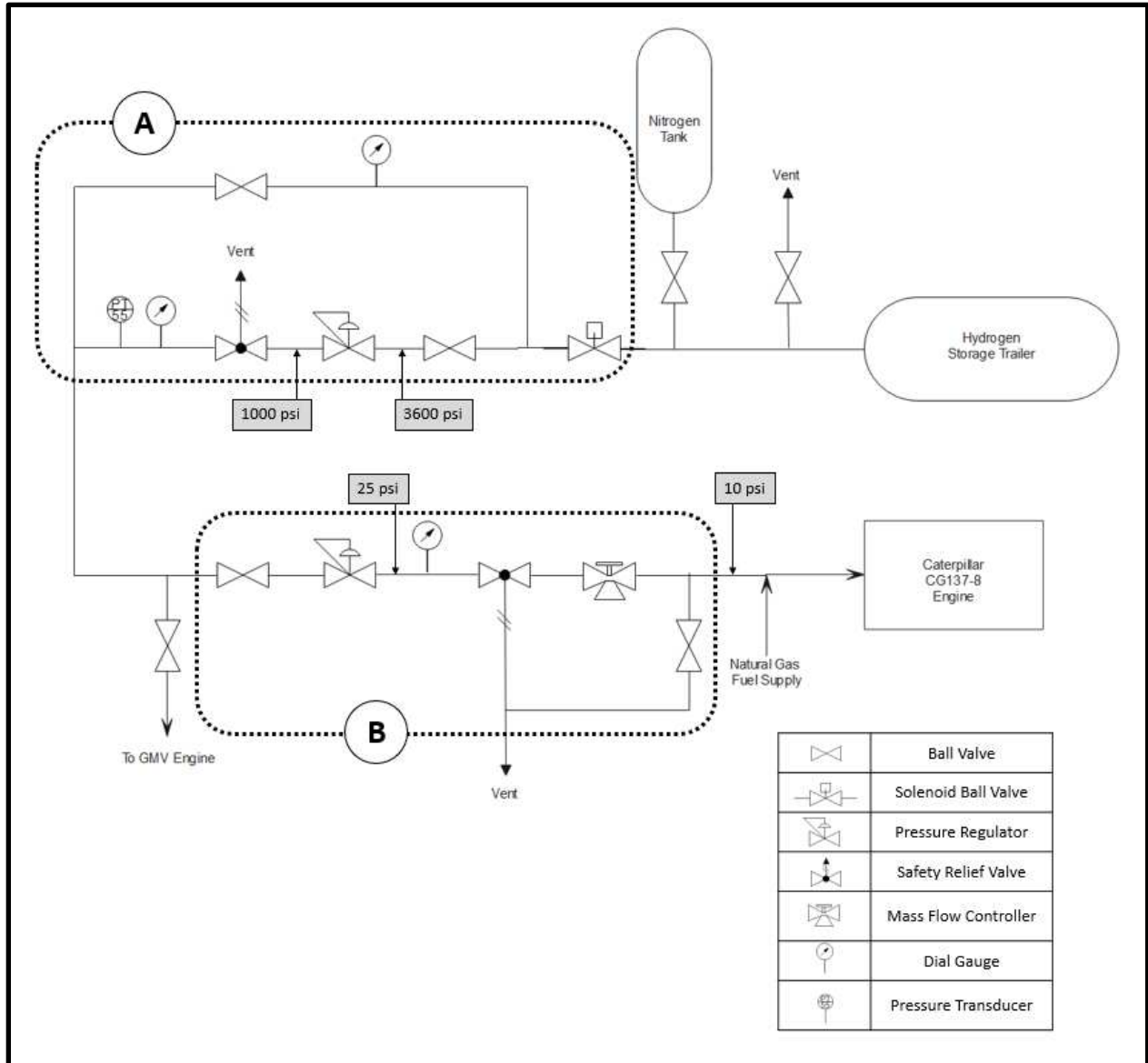


Figure B-2. Hydrogen distribution system component layout, showing the major system components as H₂ flows from the storage trailer to the CG137-8 engine. Equipment included at locations A and B shown.

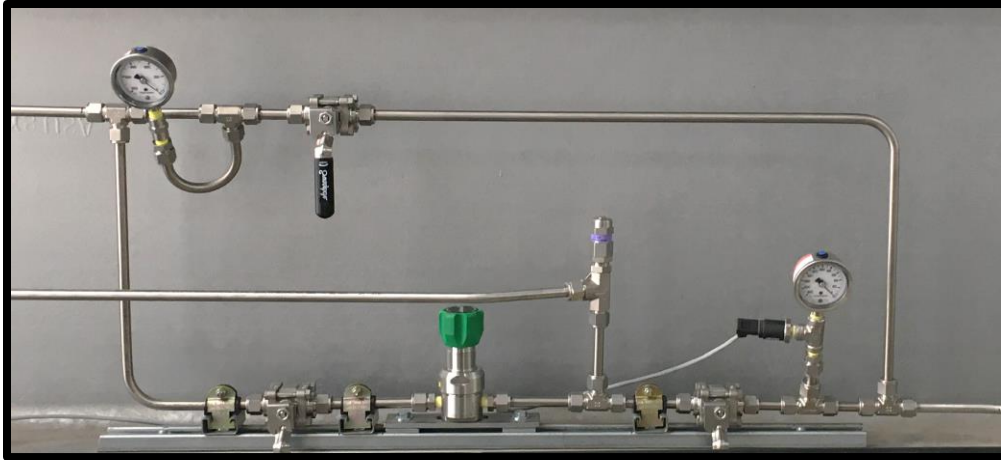


Figure B-3. Picture showing the completed regulator assembly at location A, where pressure is reduced from 3600psi down to 1000psi. The object with the green handle is the regulator, and the object with the purple band is the pressure relief valve.

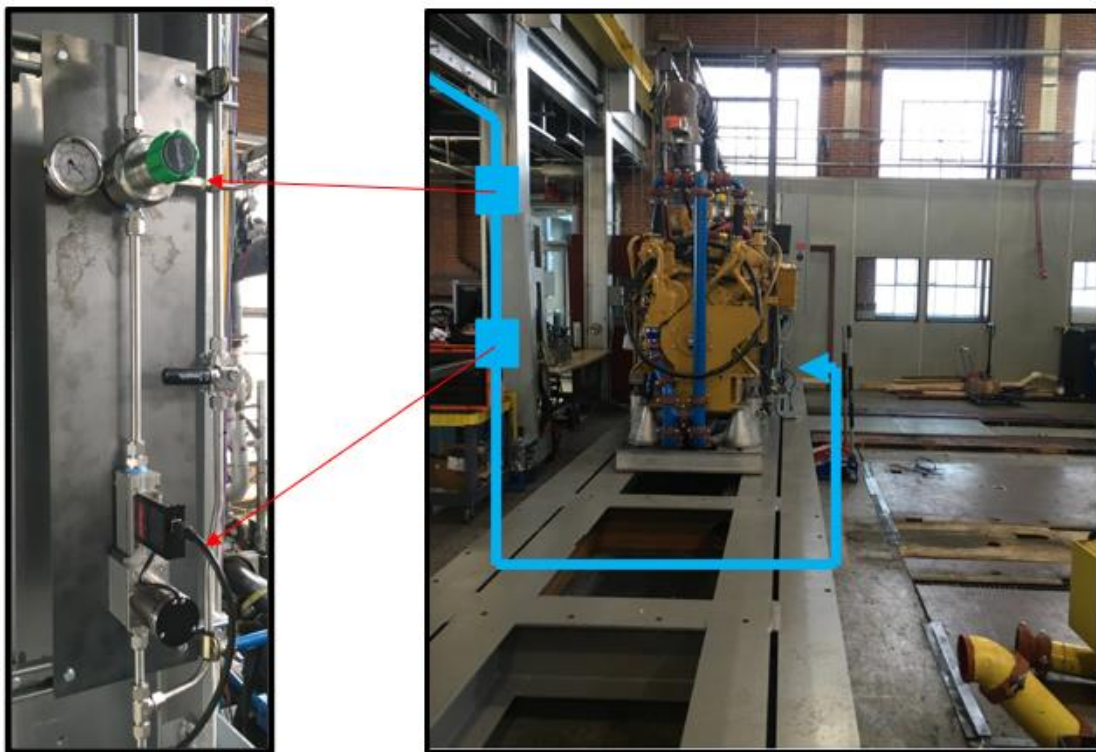


Figure B-4. Pictures showing the completed regulator assembly at location B, and its location in relation to the CG137-8 engine. The green handled item on the top is the pressure regulator, and the item pointed to below is the mass flow controller.



Figure B-5. Image on left shows the intended path of the exterior tubing, and the image on the right shows the completed exterior tubing portion.



Figure B-6. Picture showing tubing supported along the overhead by clamping to I-beams.